Frontiers in Heat and Mass Transfer (FHMT), 1, 013001 (2010)
DOI: 10.5098/hmt.v1.1.3001

Global Digital Central
ISSN: 2151-8629

Frontiers in Heat and Mass Transfer

Available at www.ThermalFluidsCentral.org

TURBINE BLADE FILM COOLING USING PSP TECHNIQUE

Je-Chin Han* and Akhilesh P. Rallabandi

Texas A&M University, College Station, Texas, 77843-3123, USA

ABSTRACT

Film cooling is widely used to protect modern gas turbine blades and vanes from the ever increasing inlet temperatures. Film cooling involves a very complex turbulent flow-field, the characterization of which is necessary for reliable and economical design. Several experimental studies have focused on gas turbine blade, vane and end-wall film cooling over the past few decades. Measurements of heat transfer coefficients, film cooling effectiveness values and heat flux ratios using several different experimental methods have been reported. The emphasis of this current review is on the Pressure Sensitive Paint (PSP) mass transfer analogy to determine the film cooling effectiveness. The theoretical basis of the method is presented in detail. Important results in the open literature obtained using the PSP method are presented, discussing parametric effects of blowing ratio, momentum ratio, density ratio, hole shape, surface geometry, free-stream turbulence on flat plates, turbine blades, vanes and end-walls. The PSP method provides very high resolution contours of film cooling effectiveness, without being subject to the conduction error in high thermal gradient regions near the hole.

Keywords:*Gas Turbine, Heat Transfer, Film Cooling, Shaped Holes, PSP*

1. INTRODUCTION

Gas turbine inlet temperatures have been increasing over the years due to positive economies of higher efficiency at higher firing temperatures. In the 1960s, material properties limited gas turbine firing temperatures and turbine blade temperatures to around 800C. Modern firing temperatures are closer to 1500C though blades (comprised of super-alloys) cannot be allowed to exceed temperatures of 900C, to minimize the negative effects of thermal stresses. This large differential in temperature between the hot gas and the blade surface results in a very significant thermal load, as represented in Fig.1. Advanced blade cooling technologies (for instance, those shown in Figs.2 are instrumental in allowing for this large thermal load. (Han *et al.* (2000)).

Advanced cooling technologies include blade internal cooling (Fig.2(b)) and external cooling (Fig.2(a)). Secondary coolant air is bled from the turbine compressor stage (typically at a much lower temperature). This air is ducted at high Reynolds numbers through cooling channels inside the blade/vane which are equipped with rib turbulators to remove heat from the blade. Channels roughened with pin-fins are used in the trailing edge region of the blade; the heavily loaded leading edge region is cooled by jet-impingement cooling.

External cooling of the turbine blade is achieved by film cooling and the provision of an insulating thermal barrier coating. Film cooling involves the secondary fluid being discharged into the hot mainstream through holes drilled into the internal cooling passages. The goal is to form an insulating film reducing contact of the blade material with the hot mainstream.

Since the thermodynamic cost of tapping air from the compressor is high, a thorough understanding of the flow-field and various parametric effects is of great value to the engine designer. Characterizing film cooling using scaled models in the laboratory has been an aggressive academic pursuit in the past few decades.

The two layer model (Fig.3) to analyze film cooling effectiveness stipulates that the cooling air exiting the film cooling holes forms an insulating layer of temperature T_f on the surface of the blade. The heat transfer between the layer and the blade surface is given by Eq.2. These parameters (η and h) are convenient to measure in scaled down laboratory tests.

For a surface without film cooling, the heat load is

$$q''_o = h_o(T_\infty - T_w) \tag{1}$$

*Corresponding author. Email: jc-han@tamu.edu.

Frontiers in Heat and Mass Transfer (FHMT), 1, 013001 (2010)
DOI: 10.5098/hmt.v1.1.3001
Global Digital Central
ISSN: 2151-8629

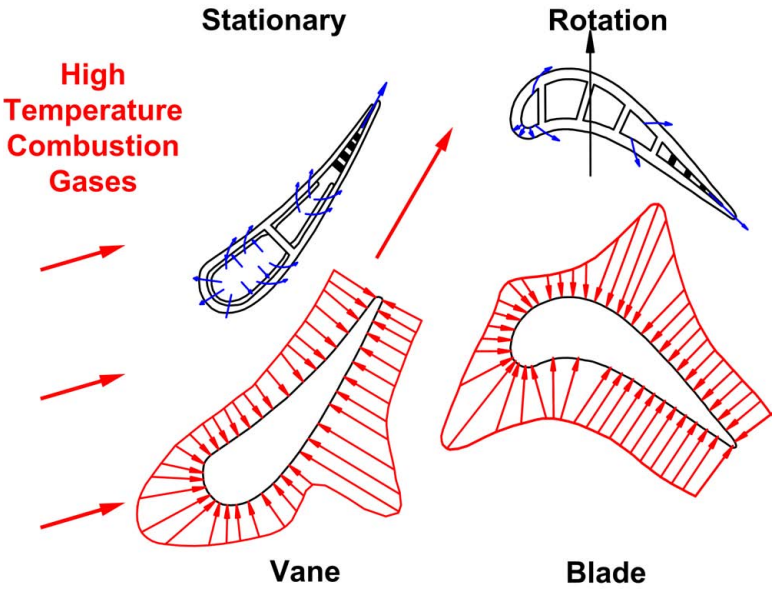

Fig. 1 Gas turbine blade thermal loading schmatic

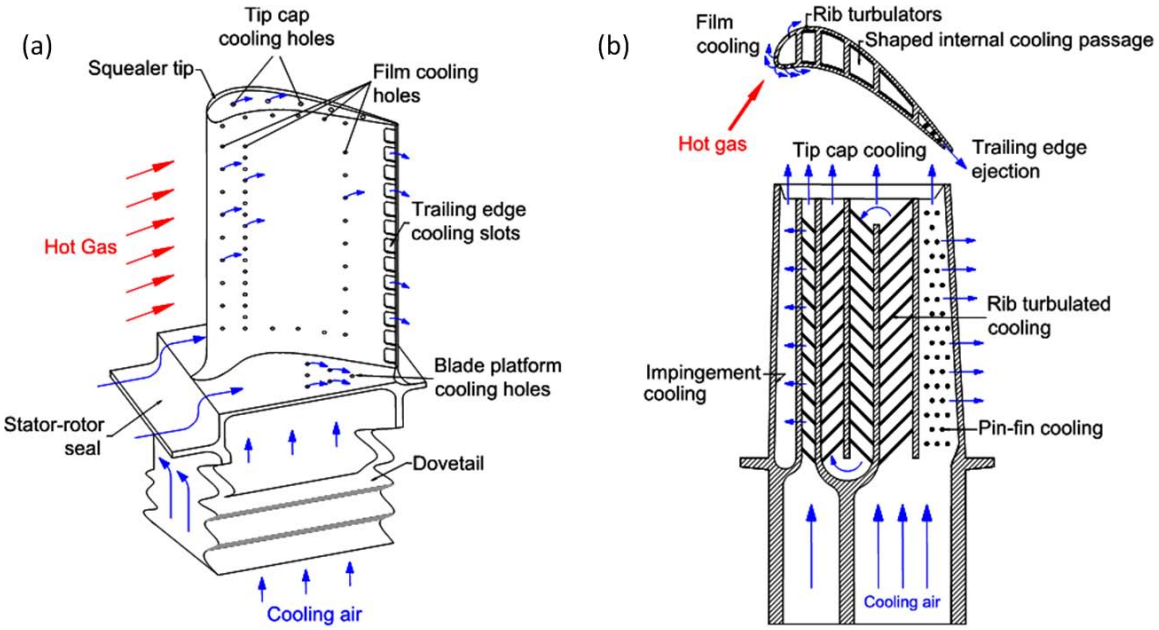

Fig. 2 Gas turbine blade cooling schematic (a) External cooling (b) Internal cooling

For a surface cooled by a film, injected at temperature T_c

$$q'' = h(T_f - T_w) \tag{2}$$

The temperature T_f dilutes progressively, downstream of the hole because the film interacts with the turbulent mainstream. The film cooling effectiveness is a non dimensional version of T_f.

$$\eta = \frac{T_\infty - T_f}{T_\infty - T_c} \tag{3}$$

If blade materials with very low conductivity can be used, then the wall temperature, T_{aw} can be used as a proxy for the film temperature, T_f. The resulting effectiveness is called 'adiabatic' effectiveness - and is identical to the film cooling effectiveness. These quantities can be combined to yield the heat flux reduction, the figure of merit relevant to the engine designer. The benefit of film cooling is realized only of this parameter is below 1.0.

$$\frac{q''}{q''_o} = \frac{h}{h_o}\left(1 - \eta\frac{T_\infty - T_c}{T_\infty - T_w}\right) \tag{4}$$

An alternative approach to assessing the performance of film cooling is the super-position approach, where heat transfer coefficients for the case *with* film cooling are calculated using the mainstream temperature as a reference rather than the film temperature. (defined by Eq.1, by measuring T_∞, T_w and q''_o). Results computed using this approach are conventionally presented using a parameter called Stanton Number Reduction (SNR).

$$SNR = 1 - \frac{St_{film}}{St_{no-film}} \tag{5}$$

Frontiers in Heat and Mass Transfer (FHMT), 1, 013001 (2010)
DOI: 10.5098/hmt.v1.1.3001
Global Digital Central
ISSN: 2151-8629

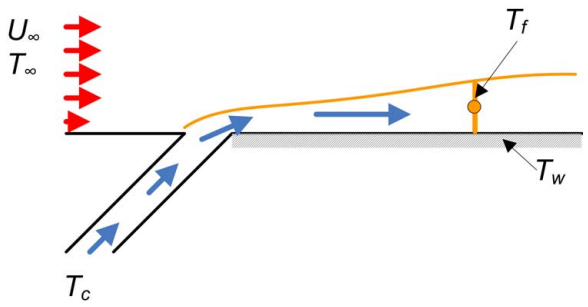

Fig. 3 Film cooling two layer model - Schematic

Both approaches are conceptually equivalent.

A detailed discussion of these models is available in Moffat (1987), Goldstein (1971), Han *et al.* (2000). The focus of this review paper is on the film cooling effectiveness only.

Over the years, a large body of literature has been generated pertinent to film cooling. Film cooling hole configurations i.e. shape, length, spacing and orientation have been studied in detail (Fig.4). Film cooling has also been found to be very sensitive to the coolant to mainstream density, momentum and mass flux ratios, the mainstream turbulence intensity, mainstream passage/tip vortices, upstream wakes, surface curvature and roughness. Film cooling is used on various components of the turbine system - the stator nozzle, the rotor blade, the end-wall and the tip - and each configuration displays different parametric sensitivities.

Thorough reviews of the parameters effecting film cooling are provided by Goldstein (1971), Han *et al.* (2000), Han and Ekkad (2001),Bogard and Thole (2006) and Bunker (2005).

Recent advances in turbulence modeling have allowed for an increasing accuracy of numerical estimates of film cooling behavior. Several recent works have used in-house and commercial CFD codes to predict film cooling flow-fields with reasonable success, using RANS as well as LES approaches.

In this paper, a brief review of various parametric effects on film cooling will be presented in the first section. Computational results will not be reviewed. The mass transfer analogy and the Pressure Sensitive Paint (PSP) based method to determine film cooling effectiveness will be discussed in the second section. A few representative results using the PSP method will then be presented.

1.1. Flat Plate Film Cooling

It is common in literature to use a flat plate to perform fundamental studies on various parametric effects on film cooling. Also, results on flat plates have been used to calibrate and standardize various experimental techniques to measure film cooling effectiveness and heat transfer coefficients.

While the best film cooling coverage can be obtained by injecting the fluid parallel to the mainstream, manufacturing constraints dictate that holes be angled. Using film cooling holes perpendicular (90^o) to the mainstream results in very low film cooling effectiveness. The use of holes inclined at 35^o typically strikes a balance between film cooling performance and manufacturing ease.

Effect of Coolant-Mainstream Blowing Ratio. Blowing ratio (M) is defined as the ratio of the coolant mass flux to that of the mainstream. In general, regardless of hole-shape and angle, film cooling effectiveness is found to increase with blowing ratio at low blowing ratios. However, beyond a critical blowing ratio, film cooling effectiveness is found to decline. This decline can be attributed to the phenomenon of *film-cooling lift-off.*, wherein the high momentum film-cooling jet fails to attach with the plate surface and penetrates into the mainstream. There is wide agreement in the literature regarding this, e.g. Goldstein *et al.* (1974); Pedersen *et al.* (1977); Sinha *et al.* (1991) and Rallabandi *et al.* (2008).

Effect of Coolant-Mainstream Density Ratio. The coolant to mainstream density ratio (DR) in modern gas-turbine engines is typically around 2.0, due to the significantly lower temperature of the coolant. Scaled down laboratory tests (to simulate engine DR conditions) usually involve chilling the coolant to very low temperatures (Sinha *et al.* (1991)) or using a foreign gas with a higher density (e.g. Goldstein *et al.* (1974), Pedersen *et al.* (1977), Du *et al.* (1997)). In general, increasing DR at a given M results in a higher effectiveness, especially at higher blowing ratios, since the momentum of a high density coolant is lower at a given M, there is a lower tendency to lift-off.

Effect of Hole Configuration. Injecting the film coolant at an angle to the mainstream (a compound angle) results in higher film cooling effectiveness, due to greater lateral diffusion of the coolant (Fig.4). Compound angled configurations are also found to resist to lift-off more than simple angled configurations, as reported by Ligrani *et al.* (1994b) and Ekkad *et al.* (1997). Using shaped film cooling holes (with a fan shaped diffuser on the blade surface) results in a smaller tendency to lift off due to the reduction in momentum due to the increase cross sectional area for the coolant, as reported by Schmidt *et al.* (1996) and Gritsch *et al.* (1998).

Embedding film cooling holes in slots (Bunker (2002)), trenches (Waye and Bogard (2007)) (to simulate thermal barrier coating sprays) and downstream of backward facing steps (Rallabandi *et al.* (2008)) has been found to increase film cooling effectiveness in the proximity of the hole.

Multiple Row Film Cooling. Multiple rows of film cooling holes are conventionally used in turbine blade designs. Ligrani *et al.* (1994a) studied typical distributions with both simple and compound angles. At lower blowing ratios, the effects of the numbers of rows is fairly insignificant. However, on increasing the blowing ratio the double jet row showed a higher effectiveness.

More recently, Kusterer *et al.* (2007) studied two rows of film cooling holes with opposite orientation and internal supply geometries. These holes resulted in higher film cooling effectiveness by canceling out the counter-rotating 'kidney' vortices (which are induced by the interaction of the inclined jet with the mainstream). Dhungel *et al.* (2007) presented measurements of film cooling effectiveness using film cooling holes supplemented with special anti-vortex holes to increase the effectiveness.

Effect of Mainstream Turbulence. Depending on the location, the mainstream turbulence intensity experienced by a row of film cooling holes varies. Film cooling holes located on the first stator vane experience turbulence intensities of up to 20%. However, due to acceleration of the mainstream in the stator nozzle, the rotor experiences lower turbulence intensities (when not under the influence of the wake or shock of the upstream stator vane,

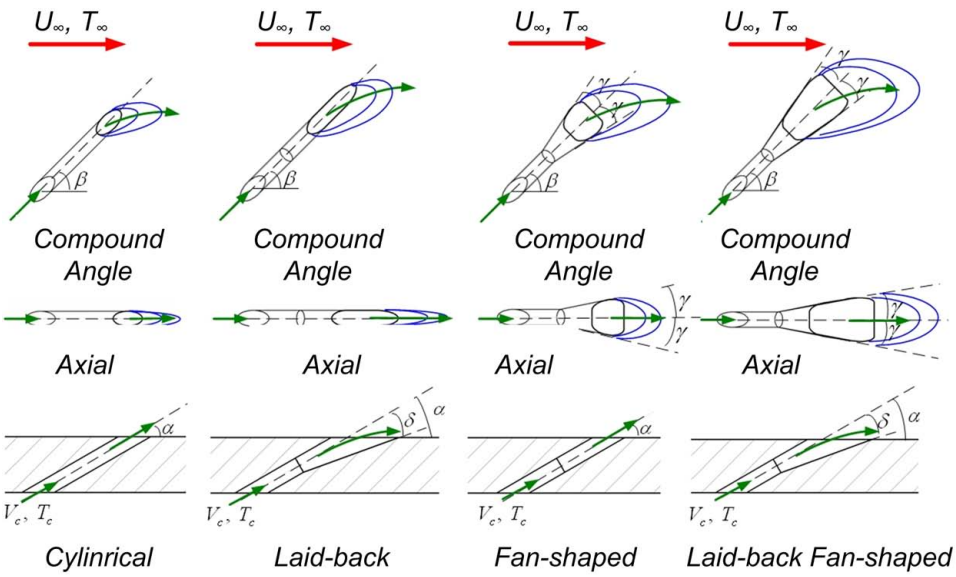

Fig. 4 Film cooling hole shape effect: Schematic

which increase local turbulence intensities significantly). Further, flow along the blade proximate to the leading edge portion is transitional rather than fully turbulent. Turbulence intensity is a therefore significant parameter in turbine blades. Free stream turbulence (simulated by grids) is found to have a monotonic effect on flat plate film cooling: film cooling effectiveness traces are found to be shorter due to mainstream turbulence, as found by Bons *et al.* (1996) and Wright *et al.* (2005).

1.2. Blade Surface Film Cooling

Film cooling on the surface of the turbine blade / vane is further complicated by surface curvature, secondary flows such as tip-leakage (Bindon (1989)) and horseshoe vortices (Goldstein and Spores (1988)) and unsteady wakes (Mayle (1991)).

Effect of Surface Curvature. The results of Ito *et al.* (1978) and Schwarz *et al.* (1991) indicate that film cooling effectiveness is relatively subdued on the concave (pressure) side in comparison with the convex (suction side), with the flat plate effectiveness values lying in between. Lift-off occurs at a lower blowing ratio on the concave side. However, the curvature of the concave surface results in a reattachment of the lifted-off coolant on the pressure side, resulting in higher downstream effectiveness. Ethridge *et al.* (2001) studied the effect of coolant-to-mainstream density ratio on a vane with high curvature.

Dittmar *et al.* (2002) studied different film cooling hole configurations on the suction (convex) side and concluded that shaped holes provide better coverage at higher blowing ratios by resisting jet penetration into the mainstream. Chen *et al.* (2001) observed an improvement in performance on the concave (pressure) surface due to using compound angled holes instead of simple angled holes at higher blowing ratios. An improvement was seen on the suction side at all blowing ratios.

Effect of Secondary Flows and Unsteady Wakes. Garg (2000) used an implementation of the $k-\omega$ model to simulate a complete film cooled blade. The effects of tip leakage vortices and horseshoe vortices on the film coolant flow-path can be seen. These vortices result in an expansion of the film coolant on the pressure side, and a contraction of the coolant trace on the pressure side, a result confirmed by future tests (Mhetras *et al.* (2007) and Narzary *et al.* (2007)).

Rigby *et al.* (1990) made measurements of heat transfer coefficients using the super-position approach on film cooled blades under the influence of an unsteady wakes and shocks from a simulated stator. These unsteady phenomena had a significant effect on the measured Stanton number reduction on the suction surface.

A rotating spoke-wheel wake generator installed upstream of a typical high pressure film cooled model turbine blade has been to simulate the effect of an upstream wake by Mehendale *et al.* (1994) and later, Du *et al.* (1997). Film cooling effectiveness on the blade surface (equipped with radial angled holes on the leading edge, two rows of simple angled holes on the suction side, and two rows of compound angled holes on the pressure side) was studied. A reduction in film cooling effectiveness due to the unsteady wake was observed across the board. Teng *et al.* (2000) used cold-wire anemometry to measure the mean and fluctuating temperature profiles within the film cooling jet. Increased turbulence in the boundary layer can be clearly observed in the unsteady wake case, which results in shorter coolant traces. The effect of the unsteady wake on film cooling effectiveness is similar to that of free-stream turbulence.

1.3. Leading Edge Film Cooling.

A large semi-cylinder is conventionally used as a good approximation to the stagnation region on a turbine blade. Initial studies into film cooling effectiveness near the leading edge were performed by Luckey *et al.* (1977). Shower-head holes inclined at different angles were tested and a correlation for the optimum blowing ratio was arrived at. Film cooling effectiveness measurements on a simulated leading edge were also presented by Mick and Mayle (1988) and Mehendale and Han (1992), showing phenomenon of jet penetration into the mainstream (*lift-off*) at high blowing ratios.

Higher resolution data was acquired by Ekkad *et al.* (1998) using the transient liquid crystal method. The deterioration of film

Global Digital Central
ISSN: 2151-8629

cooling effectiveness due to an unsteady wake in the leading edge region was studied (using a spoke wheel) by Funazaki *et al.* (1997) and Heidmann *et al.* (2001). The use of shaped holes to improve film coverage has been studied by Reiss and Bölcs (2000), Falcoz *et al.* (2006) and Gao and Han (2009).

1.4. Blade Tip Film Cooling

Film cooling on the blade tip has a dual purpose - to protect the tip by forming an insulating film, and to reduce hot-gas tip leakage from pressure side to the suction side, reducing heat transfer coefficients on the tip.

A review of the work done on tip-gap film cooling by Dr. Metzger's group is available in Kim *et al.* (1995). More recently, Kwak and Han (2003a,b) and Christophel *et al.* (2005) used thermal imaging techniques (Liquid crystal and IR thermography respectively) to measure detailed film cooling effectiveness contours on the tip with holes on the tip region of the pressure side and on the tip. The effect squealer tips (used to inhibit tip leakage) on film cooling was also studied. In general, the literature agrees that a higher blowing ratio and a lower tip clearance result in better film cooling performance.

Ahn *et al.* (2005) and Mhetras *et al.* (2008a) measured effectiveness using the PSP technique with holes on the pressure side (tip region) and the tip. Gao *et al.* (2009b) characterized the effect of blade angle-of-attack on film cooling effectiveness using the PSP technique.

1.5. Endwall Film Cooling

Due to the large difference in pressure between the pressure and suction side of the blade, secondary vortices are formed in the hub end-wall region. (Langston (1980) and Goldstein and Spores (1988)). These vortices increase heat transfer, necessitating provisions for aggressive film-cooling of the end-wall. To achieve this end, film coolant is typically ejected from the rotor-stator gap to cool the end-wall. Besides this, engine designs also incorporate discrete film cooling holes along the end-wall.

Takeishi *et al.* (1990) tested end-walls with discrete film cooling holes while Harasgama and Burton (1992) used film cooling holes near the leading edge. Jabbari *et al.* (1996) used film cooling holes placed in the downstream section of the blade passage. Friedrichs *et al.* (1996) used an innovative ammonia-diazo mass transfer analogy to measure film cooling effectiveness on the end-wall due to discrete holes.

The effectiveness corresponding to the film coolant discharged through the the rotor-stator gap has been studied by Burd *et al.* (2000), Oke *et al.* (2002) and Zhang and Jaiswal (2001). Difficult to cool areas such as the blade leading edge-end-wall junction can be cooled using this approach. The additional momentum introduced in the near wall region by the slot coolant tends to reduce the strength of the secondary flows. The effect of upstream wakes and vortices generated by stationary wake rods and delta wings was studied by Wright *et al.* (2009).

More recently, the improvement in film cooling due to the usage of shaped holes in the end-wall has been studied by Barigozzi *et al.* (2007), Colban *et al.* (2008) and Gao *et al.* (2009a). The effect of coolant density ratio on film cooling effectiveness was studied by Narzary *et al.* (2009), with the conclusion that higher density coolants are more resilient to lift-off and result in higher film cooling effectiveness.

1.6. Trailing Edge Film Cooling

A comprehensive survey of film cooling investigations prior to 1971 was done by Goldstein (1971) and included data for slots as well as discrete holes. Emphasis was on 2-dimensional slots. Taslim *et al.* (1992) found that the lip-to-slot height ratio has strong impact on film cooling effectiveness.

Martini and Schulz (2004) and Martini *et al.* (2006) measured the film cooling effectiveness and heat transfer on the trailing edge cutback of gas turbine airfoils with different internal cooling structures using the IR thermography method, showing the strong impact of internal design on the film cooling performance downstream of the ejection slot. The fast decay in film cooling effectiveness was attributed to vortex shedding from the pressure side lip. Cunha *et al.* (2006) studied the impact of trailing edge ejection on heat transfer using a closed form, analytical solution for temperature profiles for four different configurations. Chen *et al.* (2006) measured heat transfer and film cooling effectiveness on the slot floor with liquid crystal technique, finding higher heat transfer coefficient on the slots due to mixing, however, the overall heat flux reduction was high with the slot cooling.

Recently, Cakan and Taslim (2007) measured the mass/heat transfer coefficients on the trailing edge slot floor, slot sidewalls and lands using naphthalene sublimation method. They found that averaged mass transfer on the land sidewalls are higher than that on the slot floor surface. Choi *et al.* (2008) measured film cooling effectivness values for different internal cooling configurations on a cut-back trailing edge using the transient liquid method.

1.7. Film Cooling Under Rotating Conditions

Due to the difficulty of acquiring data on a rotating blade, literature studying the effect of rotation is very scarce. Dring *et al.* (1980) reported film cooling effectiveness in a rotating configuration in a low speed tunnel. Takeishi *et al.* (1992) also studied film cooling effectiveness on a stator-rotor stage, simulating a heavy duty gas turbine. Measured effectiveness values on the suction side for the rotating turbine blade seemed to match the data from the stationary cascade; whereas the rotating effectiveness on the pressure side seemed to be significantly lower than the non-rotating case. Effects of rotation are attributed to the deflection of the film cooling jet due to centrifugal forces.

Abhari and Epstein (1994) reported film cooling heat transfer coefficients by the super-position method on the short-duration MIT blow-down turbine facility using heat flux gages. Time resolved heat transfer coefficient data was obtained - and the benefit of using film cooling on the blade surface is evident.

More recently, using the PSP method, film cooling effectiveness values under rotating conditions have been measured on the leading edge by Ahn *et al.* (2006) and Ahn *et al.* (2007) and on the rotor platform by Suryanarayanan *et al.* (2009) and Suryanarayanan *et al.* (2007).

1.8. Experimental Methods

Thermal Methods.

Thermal methods involve creating a temperature differential between the mainstream and the coolant in the laboratory in order to record the film cooling effectiveness. Measurement surfaces

Global Digital Central
ISSN: 2151-8629

(blades, vanes, flat plates etc.) are typically made of a very low conductivity material to ensure that the wall surface temperature is almost equal to the film temperature. The surface temperatures are measured; knowing the mainstream and coolant temperatures, film cooling effectiveness can be estimated.

Surface temperatures can be measured by placing thermocouples at discrete locations; by using IR cameras, Thermochromic Liquid Crystals or Temperature Sensitive paint to map the temperature profile. Transient thermal methods (such as the Transient Liquid Crystal Method) making use of a semi-infinite solid assumption have to measure the film cooling effectiveness and the heat transfer coefficient simultaneously have been used.

In order to generate reliable data using thermal methods, it is imperative that the measurement surfaces be comprised of a material with *very low thermal conductivity*. In regions proximate to holes, or in regions of high film cooling effectiveness, where thermal gradient within the measurement plate is significant, a disprersion of the effectiveness data might occur.

Mass Transfer Analogy Methods.

The mass transfer analogy has been used in literature to avoid the conduction related issues. Nicoll and Whitelaw (1967) used a gas-chromatography based mass transfer analogy (sampling foreign gas at various discrete locations and estimating film cooling effectiveness). Friedrichs *et al.* (1996) used the reaction of a diazo-coated polyester film (on a turbine end-wall) with ammonia and water-vapor seeded coolant air to qualitatively and quantitatively arrive at film cooling effectiveness. Goldstein and Jin (2001) used the naphthalene sublimation mass transfer analogy (with the coolant air saturated with naphthalene) to arrive at adiabatic effectiveness.

A less cumbersome non-contact mass transfer analogy based on Pressure Sensitive Paint (PSP) has been proposed by Zhang and Fox (1999) and Zhang and Jaiswal (2001). This method has been used to arrive at detailed effectiveness contours at the Turbine Heat Transfer Lab in Texas A&M University. (e.g. Wright *et al.* (2005); Ahn *et al.* (2005); Mhetras *et al.* (2008a)). More recently, it has been possible to simulate actual engine density ratios using the PSP mass transfer analogy. (Charbonnier *et al.* (2009) and Narzary *et al.* (2009)).

This review paper will focus on the determination of film cooling effectiveness using the PSP method.

2. MEASUREMENT THEORY

2.1. Mass Transfer Analogy for Film Cooling Effectiveness

Consider the configuration shown in Fig.5(a), where a protective coolant (at T_c) is injected into a hot mainstream (at T_∞).

Governing equations for heat transfer in a two-dimensional turbulent boundary layer (in x-y co-ordinates) for a homogeneous fluid are (Kays *et al.* (2005)):

$$G_x \frac{\partial T}{\partial x} + G_y \frac{\partial T}{\partial y} = \rho(\epsilon_T + \alpha)\frac{\partial^2 T}{\partial y^2} \tag{6}$$

Here, ϵ_T is the turbulent thermal diffusivity. The adiabatic wall boundary condition (based on Fig. 5(a)) is:

$$y = 0 : \frac{\partial T}{\partial y} = 0, T = T_{aw} \tag{7}$$

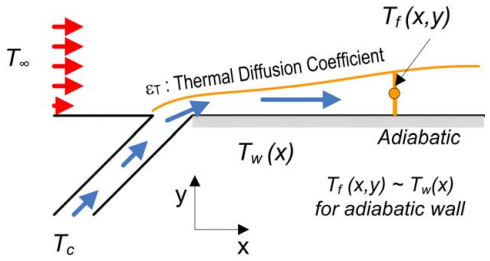

(a) Thermal boundary conditions

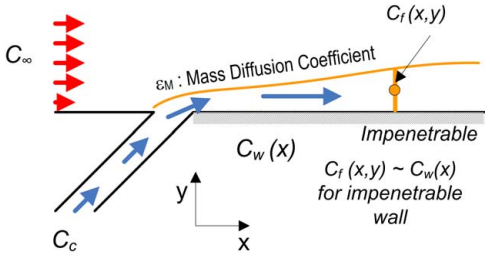

(b) Mass transfer boundary conditions

Fig. 5 Measurement of film cooling effectiveness using the heat/mass transfer analogy. Here, the y is the boundary-layer direction and x is the streamwise direction. The film temperature/concentration is a function of x,y, while wall temperatures/concentrations are functions of x only.

The mainstream temperature beyond the film is:

$$y > \delta_f : T = T_\infty \tag{8}$$

The temperature of the injected coolant:

$$x = 0 : T = T_C \tag{9}$$

Consider an analogous case, where the 'hot' mainstream has a tracer element/gas concentration of C_∞, and the coolant gas discharged through the film cooling holes has a tracer concentration of C_C, as detailed in Fig.5(b).

Corresponding governing equations for mass transfer (with C being the mass fraction either a tracer element or a component gas) are:

$$G_x \frac{\partial C}{\partial x} + G_y \frac{\partial C}{\partial y} = \rho(\epsilon_M + D)\frac{\partial^2 C}{\partial y^2} \tag{10}$$

Here, ϵ_M is the turbulent mass diffusivity. The impenetrable wall boundary condition (based on Fig. 5(b)) is:

$$y = 0 : \frac{\partial C}{\partial y} = 0, C = C_w \tag{11}$$

The corresponding concentrations of the tracer/foreign gas in the mainstream and coolant are given by:

$$y > \delta_f : C = C_\infty \tag{12}$$

$$x = 0 : C = C_C \tag{13}$$

Equations 7 and 11 reflect the analogous adiabatic wall and impenetrable wall conditions respectively. It can be noticed that

Frontiers in Heat and Mass Transfer (FHMT), 1, 013001 (2010)
DOI: 10.5098/hmt.v1.1.3001
Global Digital Central
ISSN: 2151-8629

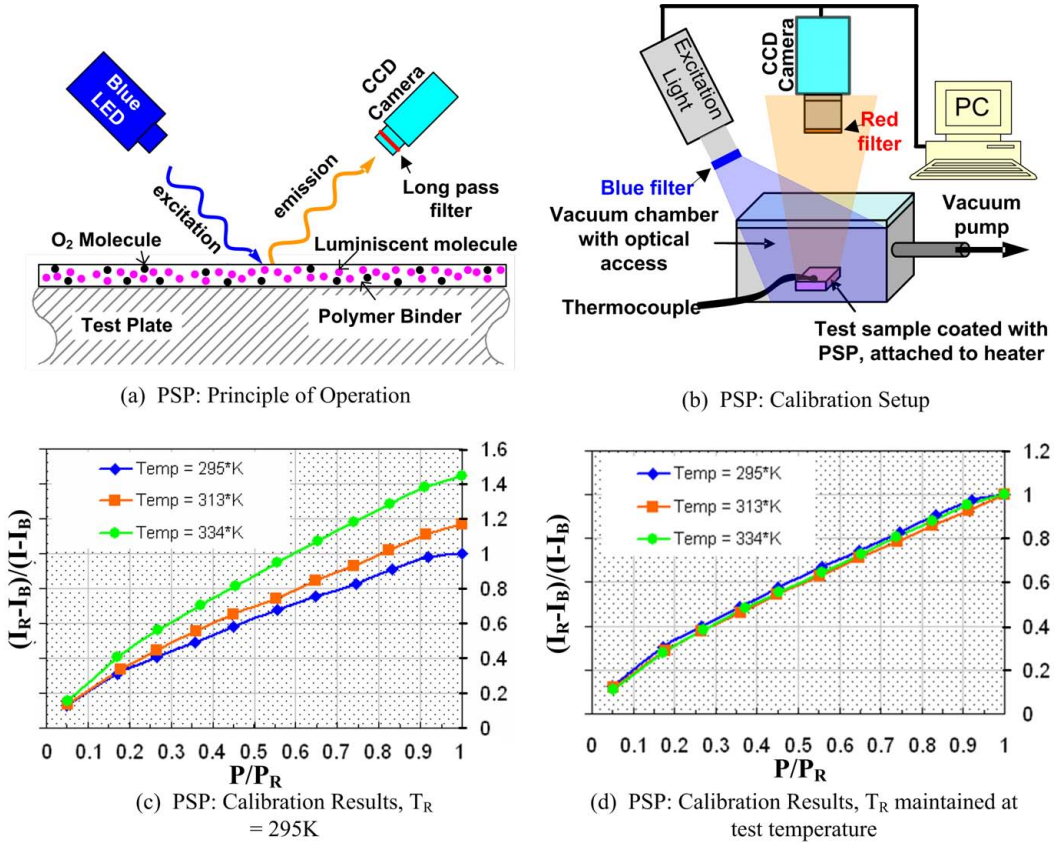

(a) PSP: Principle of Operation

(b) PSP: Calibration Setup

(c) PSP: Calibration Results, T_R = 295K

(d) PSP: Calibration Results, T_R maintained at test temperature

Fig. 6 PSP working principle, Calibration

Equations 6 and 10 and their boundary conditions have a similar structure. In the event that the turbulent Lewis number, $Le_T = \frac{(\epsilon_T+\alpha)}{(\epsilon_M+D)} = 1$, it is evident from the governing equations and boundary conditions that appropriately non dimensionalized solutions (temperatures or mass concentrations) will be identical.

Based on the work of Jones (1999) and Kays *et al.* (2005), the stipulation $Le_T \approx 1$ holds for turbulent gaseous flow fields, such as those encountered in gas turbine engines. And therefore:

$$\eta = \frac{T_f - T_\infty}{T_C - T_\infty} \approx \frac{T_{aw} - T_\infty}{T_C - T_\infty} \approx \frac{C_w - C_\infty}{C_C - C_\infty} \tag{14}$$

The underlying assumption governing the heat/mass transfer analogy ($Le_T \approx 1$) requires that the flow-field be highly turbulent. This assumption is usually valid over the surface of the gas turbine vane/blade/end-wall due to the high Reynolds numbers involved as well as various secondary mechanisms further inducing turbulence in the flow-field (such as leakage vortices, horse-shoe vortices, film cooling jets and periodic rotor/stator wakes). However, measurements have shown that the flow proximate to the leading edge portion of the blade is usually either laminar or intermittent, even with film cooling. This invalidates the governing assumption in the leading edge region, and more investigation is required to quantify this effect.

2.2. Pressure Measurement Using Pressure Sensitive Paints

Pressure sensitive paints (such as the UniFIB, composed of a blend of Fluoro Isopropyl Butyl polymer (FIB), Platinum tetra (pentafluorophyenyl) porphine (PtTFPP), and a white pigment) can be used to measure external pressure on a painted surface. When excited by a light in the blue region of the spectrum (around 400nm, usually thorough a LED array), the paint emits a light in the red region (>600nm). The excited electrons of the PSP emit a photon in the red range of the spectrum to fall back to their degenerate state. Another radiation-free path to the degenerate state is due to interaction with Oxygen molecules. This is known as *oxygen quenching*. The intensity of the emitted light reduces with an increase in concentration (i.e. partial pressure) of oxygen adjacent to the PSP layer. (Fig.6(a),(b))

The emitted light is recorded by a scientific grade CCD camera equipped with a red-filter (to ensure none of the exciting blue light is captured). The intensity of the emitted light (after correction for background noise) is related to the partial pressure of oxygen surrounding the painted surface using the Stern-Volmer equation. (Liu *et al.* (2001).)

$$\frac{I_R - I_B}{I - I_B} = A(T) + B(T)\frac{P_{O_2}}{P_{O_2,R}} \tag{15}$$

Here, I_R is a 'reference' intensity, typically corresponding with images acquired at atmospheric conditions. The corresponding (atmospheric) pressure is given by P_R, and the atmospheric oxygen partial pressure is given by $P_{O_2,R}$. I_B is the 'black' intensity - the background noise of the CCD camera, which corresponds with images acquired in a dark room. I corresponds with intensities acquired at the calibration pressure/temperature. $A(T)$ and $B(T)$ are the Stern-Volmer constants. E_{nr} is the Arrhenius activation energy for the non-radiative process; E_p is the activation energy for oxygen diffusion. R is the universal gas constant.

Global Digital Central
ISSN: 2151-8629

$$A(T) = A(T_R)\left(1 + \frac{E_{nr}}{RT_R}\left(\frac{T - T_R}{T_R}\right)\right) \quad (16)$$

$$B(T) = B(T_R)\left(1 + \frac{E_p}{RT_R}\left(\frac{T - T_R}{T_R}\right)\right) \quad (17)$$

The emitted light intensity by the pressure sensitive paint depends on both, the partial pressure of oxygen as well as the temperature of the surface. Therefore, a calibration can be performed (typically inside a vacuum chamber with optical access) to quantify the pressure and temperature sensitivity of the paint. (Fig.6(c)). Further, ensuring that the reference temperature is identical to the tested temperature allows the curves to collapse together, compensating for the temperature effect. (Fig.6(d))

Rather than evaluate the Stern-Volmer coefficients, it is often more convenient to compute a polynomial curve fit for the data. For example, at dataset such as Fig.6(d) can be correlated by the following equation:

$$\frac{P_{O_2}}{P_{O_2,R}} = 0.0059 + 0.3961\left(\frac{I_R(T) - I_B}{I(T) - I_B}\right) + 0.9034\left(\frac{I_R(T) - I_B}{I(T) - I_B}\right)^2 - 0.3002\left(\frac{I_R(T) - I_B}{I(T) - I_B}\right)^3 \quad (18)$$

Eq.18 relates the partial pressure of oxygen to the recorded intensities. Since the molar concentration of oxygen in air is constant at 21%, the parital pressure ratio $\frac{P_{O_2}}{P_{O_2,R}}$ is identical to $\frac{P}{P_R}$. So, based on the above equation (Eq.18), one can convert recorded intensities to pressures inside a wind tunnel. However, if a foreign gas is introduced into the wind tunnel, the molar composition of the mixture changes - and the oxygen partial pressure is no longer in constant proportion to the pressure inside the wind tunnel. This property is utilized in determining the film cooling effectiveness using PSP mass transfer analogy.

2.3. The PSP Mass Transfer Analogy to Determine Film Cooling Effectiveness

The PSP method to determine film cooling effectiveness is fairly insensitive to the material of the base plate. Any rigid (non-deforming) material impervious to oxygen will suffice. The pressure sensitive paint is applied to the region of interest, which typically includes the region around and up to 30-40 diameters downstream of the film cooling holes. In the case of full-coverage film cooling, the entire blade surface can be coated with the PSP. A base layer of black acrylic paint is applied to the surface before the PSP is sprayed. The PSP is carefully sprayed using an airbrush. Care is taken to ensure that the PSP is sprayed uniformly - and that the layers are amply thick. Over-spraying might result in thick layers of the paint peeling off from the surface.

Various foreign gases are injected through the film cooling holes to simulate the coolant-to mainstream density ratio effect. The foreign gas reduces the local concentration of oxygen near the wall in regions of finite film cooling effectiveness. The PSP senses this change in concentration. A relation between the local defect in oxygen concentration and film cooling effectiveness can be arrived at.

To determine film cooling effectiveness for a given configuration, four tests are required. In each test, several images are

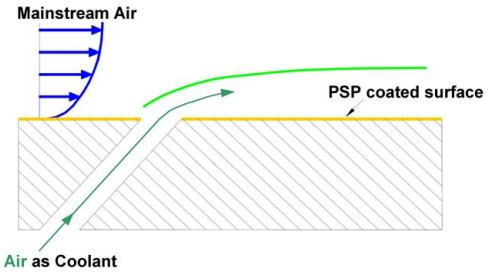

(a) Test with air used as coolant

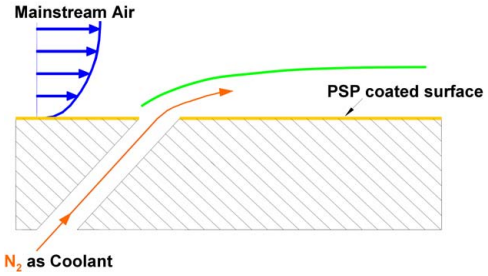

(b) Test with foreign gas (here, nitrogen) used as coolant

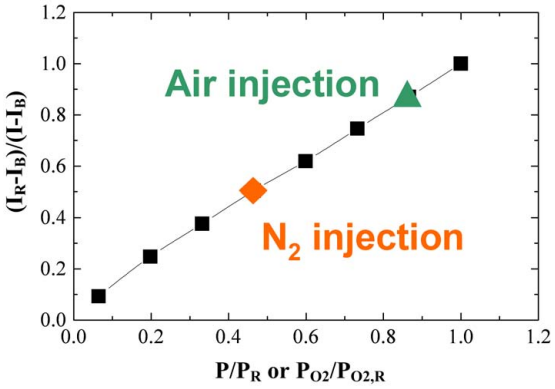

(c) Typical intesities recorded with air and nitrogen injection

Fig. 7 Measurement of film cooling effectiveness using the PSP analogy method.

captured and averaged to reduce random noise. Test 1 involves switching off the excitation LED light and capturing an image in a dark room to determine the background noise intensity. The corresponding intensity field is called I_B. Test 2 involves turning on the excitation light, focusing the camera on the region of interest and acquiring a set of images without turning on the mainstream (I_R). Test 3 (Fig.7(a)) involves establishing mainstream and coolant flow rates at the appropriate blowing ratio using air as a coolant and acquiring a set of images, (I_{air}). The resulting oxygen partial pressure and concentration fields are $P_{O_2,air}$ and $C_{O_2,air}$. Finally, test 4 (Fig.7(b)) is conducted, establishing the desired blowing ratio using the foreign gas as a coolant (nitrogen injection shown in Fig.7(b))), with the averaged intensity recorded as I_{fg}. Corresponding oxygen partial pressure and concentration fields are $P_{O_2,fg}$ and $C_{O_2,fg}$.

The expression in Eq. 14, based on the foreign-gas mass transfer analogy relates the mass fractions of oxygen with film

cooling effectiveness. An equivalent expression based on partial pressures of oxygen is sought in order to allow the application of the PSP based mass-transfer analogy.

For the air injection case, (Test 3), $C_{O_2,air}$(=$C_{O_2,\infty}$) is a constant value, since air is composed of 21% O_2 by volume. Injecting foreign gas (nitrogen injection shown in Fig.7(b))) through film cooling holes (Test 4), reduces the local mass concentration of oxygen inside the film ($C_{O_2,fg}$), resulting in a higher emitted intensity (Fig.7(c)). Also, in the test where foreign gas is injected, $C_{O_2,C} = 0$. Eq.14 becomes:

$$\eta \approx \frac{C_w - C_\infty}{C_C - C_\infty} = \frac{C_{O_2,fg} - C_{O_2,air}}{C_{O_2,C} - C_{O_2,air}} = 1 - \frac{C_{O_2,fg}}{C_{O_2,air}} \quad (19)$$

In the special case where the molecular weight of the foreign gas is similar to that of air (e.g. nitrogen injection), the mass fraction ratio equals the mole fraction ratio, which in turn equals the partial pressure ratio. This yields:

$$\eta \approx 1 - \frac{C_{O_2,fg}}{C_{O_2,air}} = 1 - \frac{P_{O_2,fg}}{P_{O_2,air}} = 1 - \frac{P_{O_2,fg}/P_{O_2,R}}{P_{O_2,air}/P_{O_2,R}} \quad (20)$$

Eq. 20 can be used to estimate the film cooling effectiveness when nitrogen is injected through the film cooling holes, converting the intensities recorded in tests 1 through 4 to partial pressures of oxygen using Eq.18 (Fig.7(c)). Several papers have been published using this methodology. (e.g. Zhang and Jaiswal (2001), Mhetras *et al.* (2007), Ahn *et al.* (2006)). When a coolant with a different density is injected through the film cooling holes (to simulate realistic density ratios), the above equation needs to be modified.

In the following equations, the mole fraction is given by X. $X_{O_2,air}$ represents the mole fraction of oxygen in air. The values of $X_{O_2,air}$ and $C_{O_2,air}$ are constant for air, regardless of absolute pressure and temperature. However, when a foreign gas (e.g. Nitrogen, Carbon Dioxide or Argon) is injected through the film cooling holes, a local variation in these values occurs inside the film. In this case, the local oxygen molar and mass concentrations are respectively, $X_{O_2,fg}$ and $C_{O_2,fg}$. Also in the foreign gas injection case, the chemical composition of the film changes the effective local molecular weight. The local effective molecular weight of the film is $W_{mix,fg}$. For the air injection case, the fluid has a constant molecular weight throughout of W_{air}.
Starting from Eq.19,

$$\begin{aligned} \eta = 1 - \frac{C_{O_2,fg}}{C_{O_2,air}} &= 1 - \frac{X_{O_2,fg}(W_{O_2}/W_{mix,fg})}{X_{O_2,air}(W_{O_2}/W_{air})} \\ &= 1 - \frac{X_{O_2,fg}W_{air}}{X_{O_2,air}W_{mix,fg}} \end{aligned} \quad (21)$$

The unknown molecular weight of the air-coolant mixture inside the film, $W_{mix,fg}$ can be related to the molecular weights of the component gases using by their mole fractions:

$$\begin{aligned} W_{mix,fg} &= X_{O_2,fg}W_{O_2} + X_{N_2,fg}W_{N_2} + X_{fg,fg}W_{fg} \\ &= X_{air,fg}W_{air} + X_{fg,fg}W_{fg} \end{aligned} \quad (22)$$

because the effective molecular weight of air, W_{air} is defined to be:

$$X_{O_2}W_{O_2} + X_{N_2}W_{N_2} = X_{air}W_{air} \quad (23)$$

Oxygen constitutes 21% of atmospheric air by volume (and hence by mole). So, $X_{air,fg} = 4.76X_{O_2,fg}$.
Since all mole fractions must add up to unity,

$$\begin{aligned} X_{O_2,fg} + X_{N_2,fg} + X_{fg,fg} &= X_{air,fg} + X_{fg,fg} \\ = 4.76X_{O_2,fg} + X_{fg,fg} &= 1 \end{aligned} \quad (24)$$

Solving for the unknown $W_{mix,fg}$ in terms of the mole fractions of oxygen, Eq 22 becomes:

$$W_{mix,fg} = 4.76X_{O_2,fg}W_{air} + (1 - 4.76X_{O_2,fg})W_{fg} \quad (25)$$

Substituting for $W_{mix,fg}$ in Eq.21 and, solving for η in terms of only one unknown

$$\begin{aligned} \eta &= 1 - \frac{X_{O_2,fg}W_{air}}{X_{O_2,air}(4.76X_{O_2,fg}W_{air} + (1 - 4.76X_{O_2,fg})W_{fg})} \\ &= 1 - \frac{1}{(4.76X_{O_2,air} + (\frac{X_{O_2,air}}{X_{O_2,fg}} - 4.76X_{O_2,air})\frac{W_{fg}}{W_{air}})} \end{aligned} \quad (26)$$

Noting that $4.76X_{O_2,air} = X_{air,air} = 1$ and that the ratio of partial pressure of a constituent chemical to the static pressure is identical to the mole fraction of the component (i.e. $X_{O_2,fg} = \frac{P_{O_2,fg}}{P}$ where P is the static pressure).

$$\begin{aligned} \eta &= 1 - \frac{1}{(1 + (\frac{X_{O_2,air}}{X_{O_2,fg}} - 1)\frac{W_{fg}}{W_{air}})} \\ &= 1 - \frac{1}{(1 + (\frac{P_{O_2,air}/P_{O_2,R}}{P_{O_2,fg}/P_{O_2,R}} - 1)\frac{W_{fg}}{W_{air}})} \end{aligned} \quad (27)$$

In the above equation (Eq.27), $P_{O_2,air}/P_{O_2,R}$ and $P_{O_2,fg}/P_{O_2,R}$ correspond with pressures calculated from the intensity fields measured by test 3 and test 4 respectively. This expression (Eq.27) was originally derived by Charbonnier *et al.* (2009), and has been used by Narzary *et al.* (2009) and Rallabandi *et al.* (2010). In the case $W_{fg}/W_{air} = 1$, Eq.27 reduces to Eq.20.

2.4. Errors and Uncertainties

Errors in reported film cooling effectiveness for a given flow rate of coolant are discussed below.

Optical Issues. While running the test, it should be ensured that the intensity of the excitation light (e.g. blue LED) is as uniform as possible. Further, the average intensity value at the reference (atmospheric) condition should be amply high, and the CCD camera should be amply sensitive so as to resolve low positive and negative gage pressures.

The major uncertainty in film cooling effectiveness stems from the resolution of the PSP (which is typically < 0.05bar). Therefore, at lower values of $\eta < 0.1$, the PSP method typically

Global Digital Central
ISSN: 2151-8629

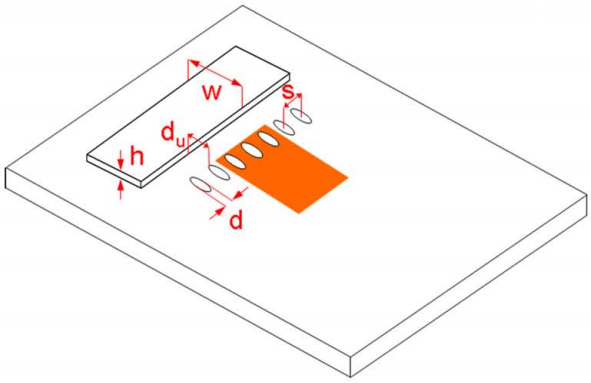

(a) Various upstream step parameters tested

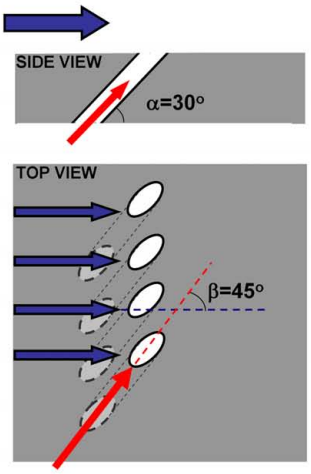

(b) Definition of compound angle

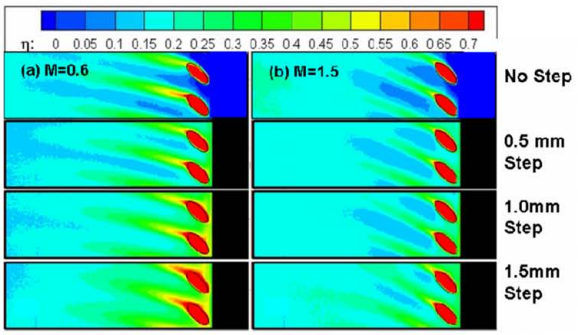

(c) Parametric effect of upstream step on cylindrical compound angled holes

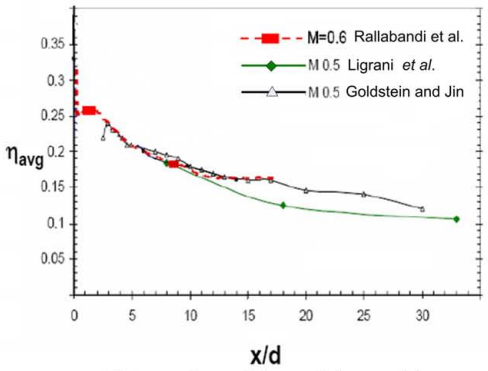

(d) Benchmarking of data with open literarture: Ligrani *et al.* (1994b) and Goldstein and Jin (2001)

Fig. 8 Flat plate film cooling from Rallabandi *et al.* (2008)

has a larger error specification $\approx 15\%$. At higher effectiveness values $\eta > 0.6$, the error is less than 5%.

Errors due to random camera noise and minor fluctuations in excitation light intensity are corrected for by computing pressures based on an average of several images (typically 200). A 'black' image, wherein camera intensities are recorded without any excitation light (in a dark room) is used to cancel out any constant-offset camera noise.

Calibration. The calibration of the PSP (Fig. 6(d)) is fairly repeatable, and several data points are usually recorded to compute a best-fit polynomial. The maximum deviation of recorded data from the best-fit curve is usually less than 1-2%. Calibration is therefore not a significant source of error. However, care must be taken to ensure that the coat of paint used to acquire data is not more than a month old, as the paint tends to photo-degrade with time, and the calibration might possibly drift with time.

Displacement of Model. Since film cooling effectiveness is often calculated on heavily loaded rotor blades / stator vanes, it is possible that the area of interest (blade surface, for instance) undergoes a deformation due to bending or rigid motion. The blade configuration of the reference image (wind-off) is therefore different from that of the air/foreign gas injection wind-on cases. The recorded image in the latter case will be a shifted version of the former case. A pixel-shift correction needs to be implemented to ensure that the reference image geometry is identical to the wind-on image geometry.

Sensitivity of PSP to Temperature. Often, it is impossible to ensure that the entire test blade is isothermal - especially when the mainstream flow in consideration is compressible, or powered by a blower in a forced-draft configuration. Based on Fig.6(c) and (d), it is evident that the reference image must be captured at the test temperature rather than the room temperature. This is achieved by capturing the reference image immediately after the test has been completed. Further, it should be ensured that the secondary air / foreign gas is also at the same temperature as the mainstream.

Mass Transfer Analogy Limitations. The mass transfer analogy holds only when the turbulent Lewis number $Le_T = 1$. This is usually a good approximation for turbulent flow. However, if the flow is laminar, then the molecular Lewis number can deviate from unity ($Le_{O_2} \approx 1.06$).

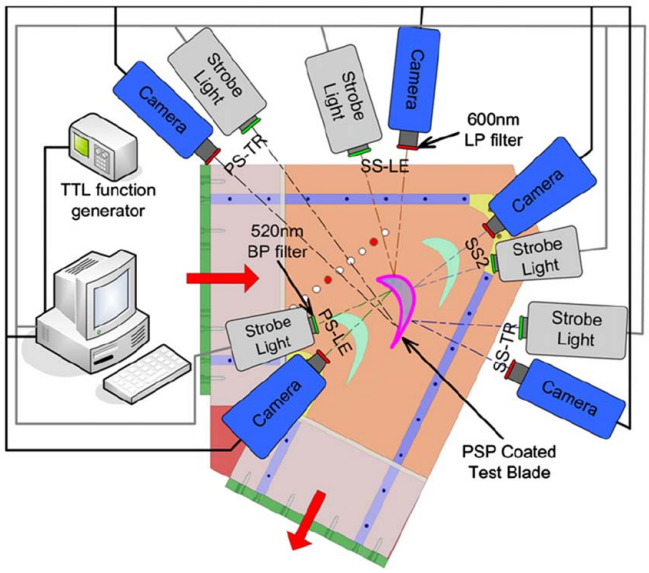

Fig. 9 Light and camera setup to capture full-blade coverage film cooling used by Mhetras *et al.* (2007)

3. RESULTS

3.1. Flat Plate

Wright *et al.* (2005) studied film cooling effectiveness downstream of a single row of holes on a flat plate and compared the PSP method with thermal methods (such as IR and TSP). Mainstream turbulence (simulated by a grid) was found to have a negative effect on film cooling effectiveness.

Rallabandi *et al.* (2008) studied the effect of a backward facing step upstream of a row of discrete film cooling holes. Simple ($\alpha = 35^o$) and compound angled ($\beta = 45^o$) cylindrical and shaped holes were studied. The hole spacing was 3.5 diameters, and the length to diameter ratio of the holes was close to 7. The area of interest (which extended up to 30 diameters downstream of the row of film cooling holes) was painted with PSP. Backward facing steps of up to 25% the diameter of the film cooling holes were studied. The mainstream turbulence level studied was 0.5%. The coolant to mainstream density ratio was 1.0, since Nitrogen was used as the coolant. Blowing ratios studied ranged from 0.3 to 1.5.

Results (Fig.8) confirmed classical trends: increasing the blowing ratio resulted in the film cooling jet lifting off from the plate surface. Compound angled holes showed a higher effectiveness than simple angled holes. Shaped holes were more resistant to lift-off than cylindrical holes. It was also observed that the backward facing step placed upstream of the row of film cooling holes resulted in higher film cooling effectiveness in the proximity of the hole. This was due to coolant getting entrapped into the recirculation zone downstream of the step.

The measured film cooling effectiveness from the cylindrical compound angled holes compare well with the results from similar tests available in open literature (Fig. 8). Goldstein and Jin (2001) used the naphthalene sublimation mass transfer analogy with simple angle, $\alpha = 35^o$ and compound angle, $\beta = 45^o$, similar to the conditions of Rallabandi *et al.* (2008). The mainstream turbulence intensity was also 0.5%. The hole spacing is also similar at 3d. Ligrani *et al.* (1994b) used a thermal method to record their data, with a spacing of 6d between the holes, $\alpha = 24^o$ and $\beta = 50^o$.

3.2. Blade Surface

Several studies have been conducted using PSP to characterize full coverage film cooling on the blade surface (e.g. Mhetras and Han (2006); Mhetras *et al.* (2007, 2008b); Narzary *et al.* (2007); Gao *et al.* (2008, 2009c)). Tests involve covering the entire blade surface with a layer of PSP. Different camera angles (e.g. Fig.9) are compiled together to yield composite blade full coverage film cooling effectiveness data. Some of these camera angles are inclined - and require the use of perspective correction algorithms to yield two-dimensional effectiveness contours.

Figures 10 and 11 show film cooling effectiveness measured by Gao *et al.* (2008) and Gao *et al.* (2009c). A typical high pressure power generation turbine blade equipped with axial laid-back fan-shaped holes (expansion and diffusion angles of 10^o) and another with compound angled laid-back fan-shaped holes are considered. The axial case (Gao *et al.* (2008)) has a stream-wise angle $\alpha = 35^o$. The compound angled case (Gao *et al.* (2009c)) has a stream wise angle of 45^o and a compound angle of 45^o. The holes are staggered in arrangement.

The model blades are comprised of a resin grown using the Stereo-Lithography (SLA) process. (One of the benefits of the PSP method is that it is not sensitive to the substrate material). Blowing ratios tested range from M=0.4 to 1.5 on both pressure and suction sides. The coolant to mainstream density ratio tested was 1.0, since nitrogen was used as the coolant. The inlet Mach number was maintained at 0.27, while the exit Mach number was 0.44.

Figures 10 and 11 also show the dependence of film cooling effectiveness on the blowing ratio. As expected, the coolant traces on the suction side are much longer than those on the pressure side (compensated by the larger number of rows on the pressure side). For the axial holes, increasing the blowing ratio results in film-cooling lift off (with an optimum blowing ratio occurring at around 0.9). The compound angled holes, in general, resulted in a higher film cooling effectiveness than the axial holes. Also, in the compound angled case, film cooling effectiveness increases with blowing ratio for the range studied. Also evident here is the effect of secondary hub and tip vortices, which create a convergence of coolant traces on the suction side, and a divergence on the pressure side, consistent with the numerical predictions of Garg (2000).

The effects of coolant-to maninstream density ratio and mainstream turbulence intensity have been studied by Narzary *et al.* (2010) for a high pressure turbine blade. The inlet Mach number is 0.23 and the exit Mach number is 0.44. A blade with cylindrical compound angled holes has been used. Density ratios ranging from 1.0 to 2.5 have been studied. Conclusions regarding the effect of density ratio (Fig.12) are similar to those reached by Rallabandi *et al.* (2010) (Fig.13(b)). Futher, increasing the mainstream turbulence intensity from 4.2 % to 10% results in a weakening of secondary flow structures.

The effect of coolant to mainstream density ratio and an unsteady stator wake (simulated by a radial spoke-wheel) was studied by Rallabandi *et al.* (2010). Rotating spokes of 9.3mm dia were used to simulate the relative motion of a stator vane up-

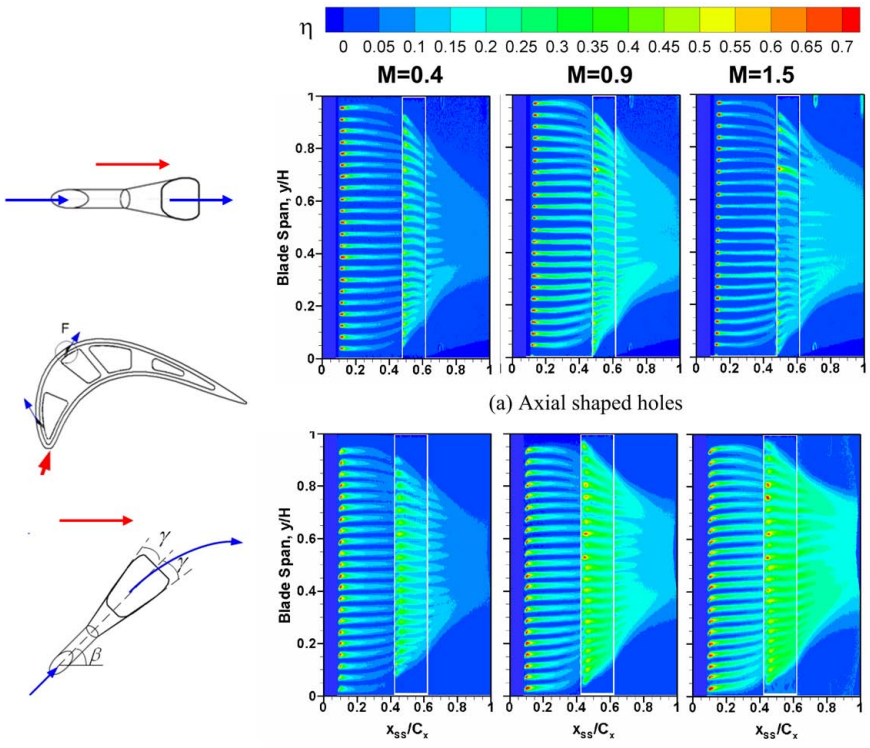

(a) Axial shaped holes

(b) Compound angled shaped holes

Fig. 10 Measured film cooling effectiveness on blade suction surface using axial and compound angled fan shaped holes from Gao *et al.* (2008) and Gao *et al.* (2009c)

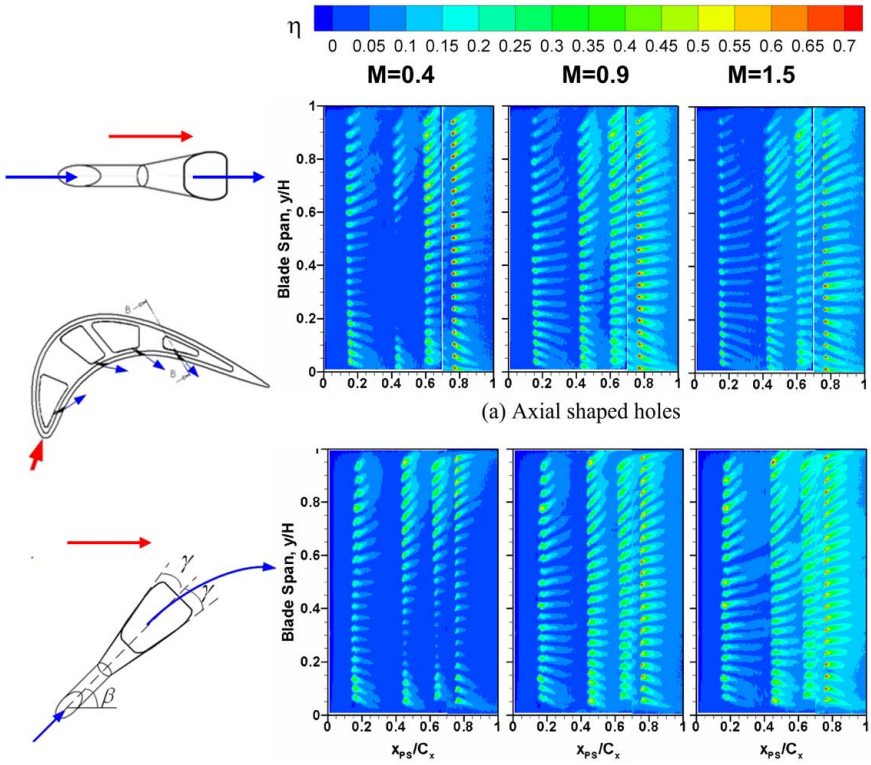

(a) Axial shaped holes

(b) Compound angled shaped holes

Fig. 11 Measured film cooling effectiveness on blade pressure surface using axial and compound angled fan shaped holes Gao *et al.* (2008) and Gao *et al.* (2009c)

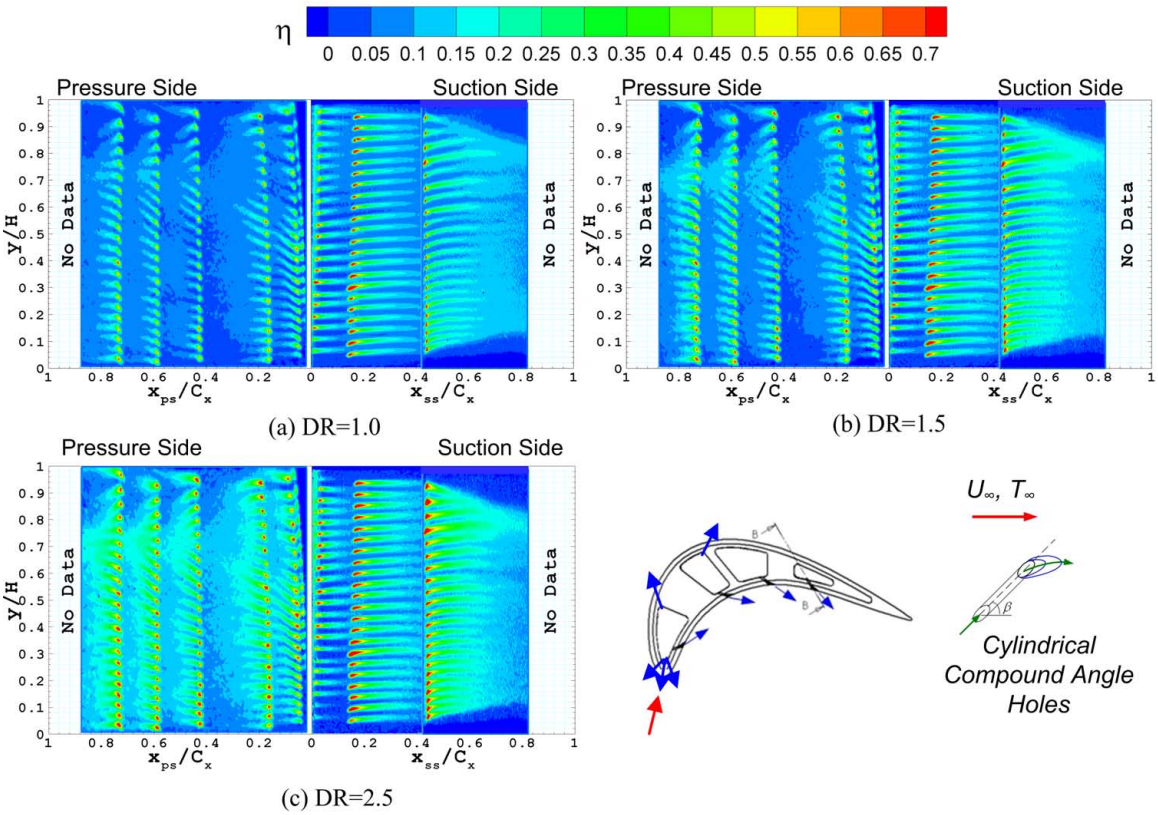

Fig. 12 Coolant to mainstream density ratio on measured film cooling effectiveness on surface using axial and compound angled cylindrical holes by Narzary *et al.* (2010)

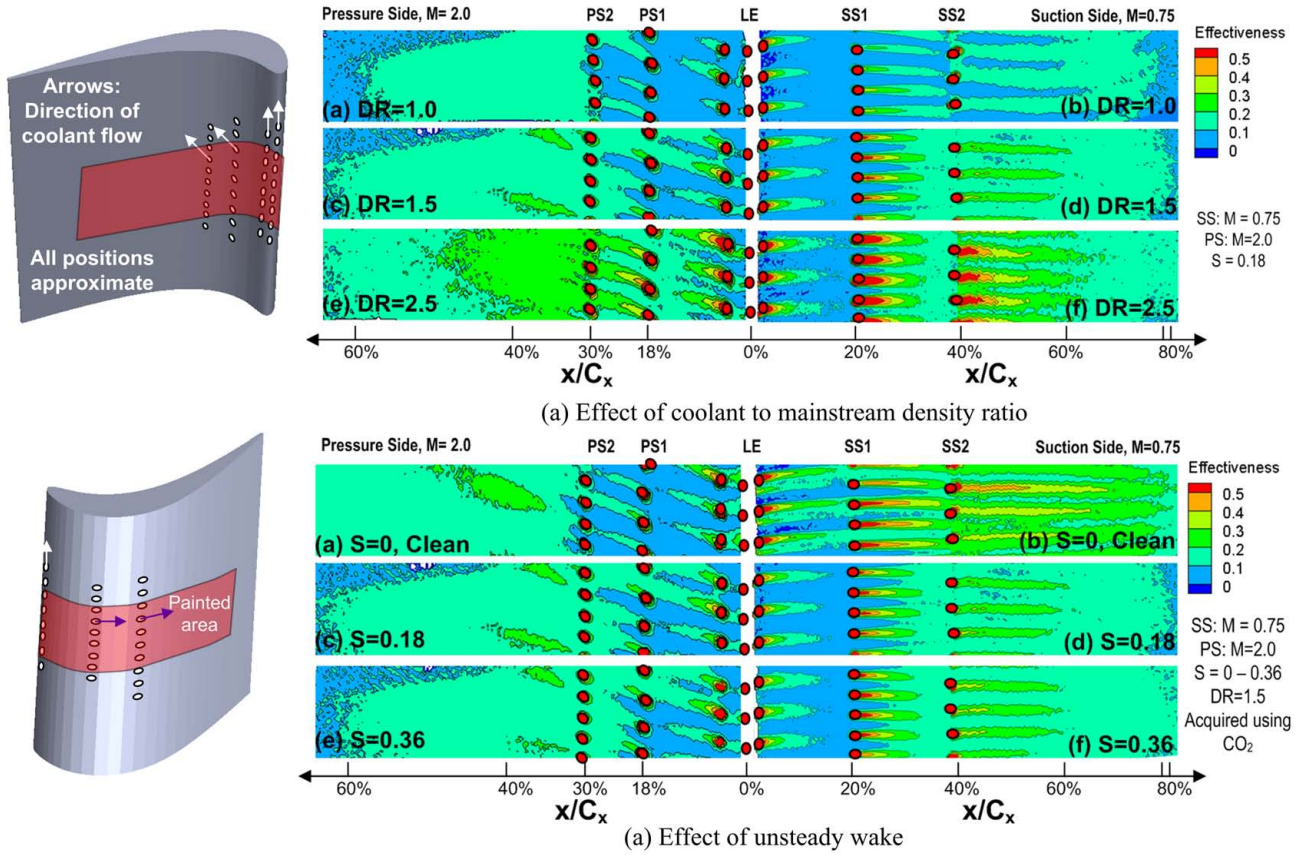

Fig. 13 Results from Rallabandi *et al.* (2010) on blade surface

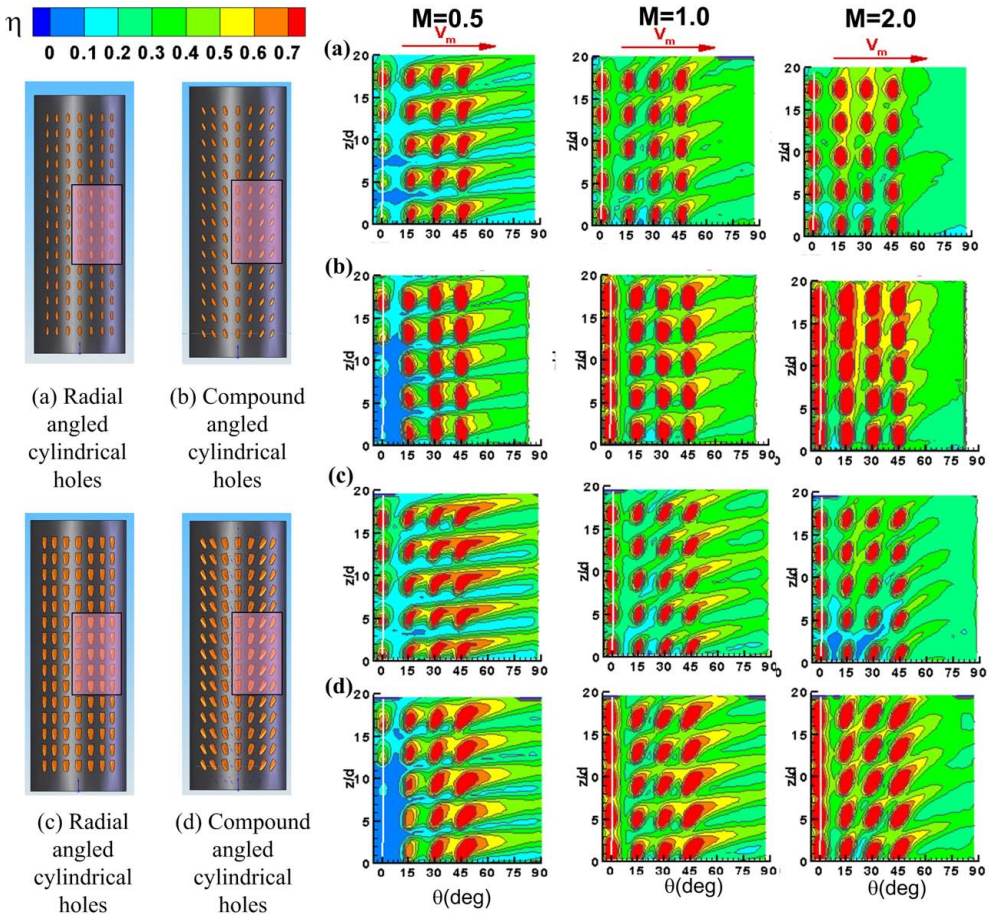

Fig. 14 Results from Gao and Han (2009) on leading edge

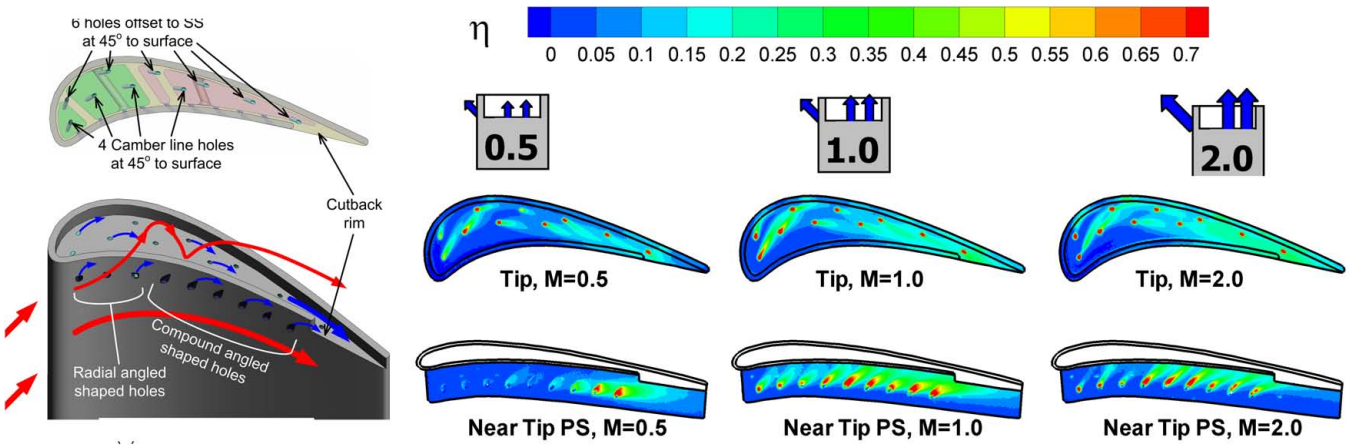

Fig. 15 Film cooling effectiveness recorded by Mhetras *et al.* (2008a) for a tip-gap ratio of 2.1%

stream of a row of heavily loaded turbine rotor blades. Simple angled holes were used on the suction side and compound angled holes were used on the pressure side. The inlet velocity was 18m/s, resulting in an exit velocity of 47m/s. Emphasis of this study was on the mid-section of the blade, which was painted with PSP. Foreign gases with variable density (Nitrogen for DR = 1.0, CO_2 for DR = 1.5 and a mixture of Ar + SF_6 for DR = 2.5) were used to simulate realistic engine density ratios. Strouhal numbers ($S = 2\pi Nnd/60v_1$ where N is the number of rods, n is the rotating speed (rpm), d is the diameter of the wake-rod and v_1 is the inlet velocity to the cascade) simulated range from 0 for the no-wake case to 0.36 for the highest RPM case.

Results show a longer coolant trace on the suction side compared with the pressure side. Due to the concave geometry of the pressure side, at higher blowing ratios, a reattachment of the lifted off jet is observed. An increase in effectiveness at higher density ratios for a given blowing ratio is observed (Fig.13), in line with existing literature. Results also showed a deterioration

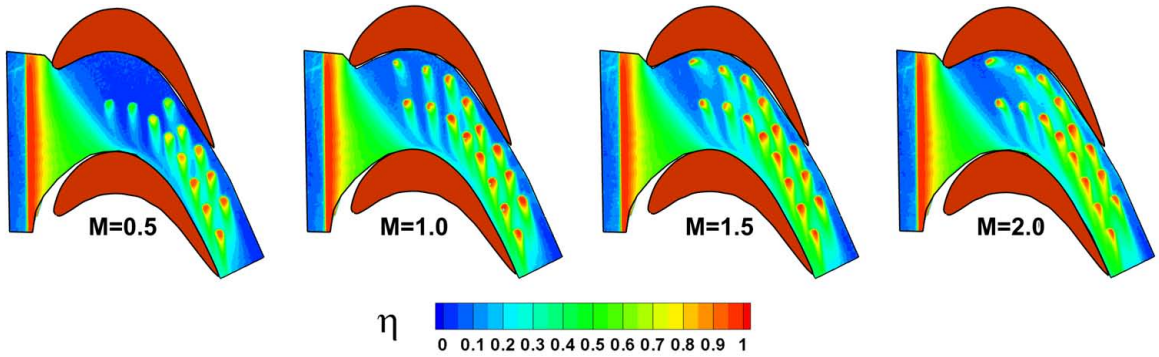

Fig. 16 Film cooling effectiveness in the hub region, from Gao *et al.* (2009a)

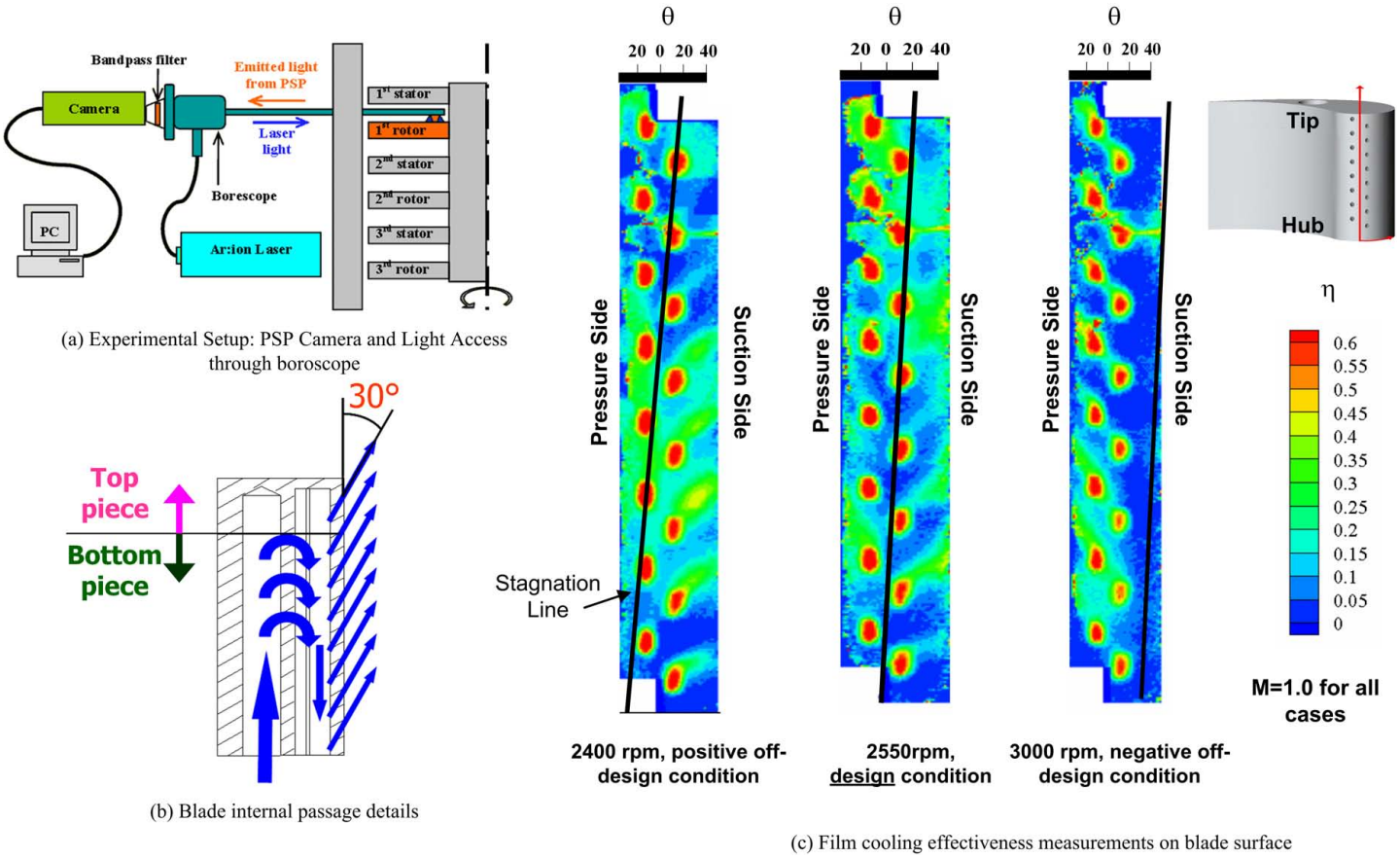

(a) Experimental Setup: PSP Camera and Light Access through boroscope

(b) Blade internal passage details

(c) Film cooling effectiveness measurements on blade surface

Fig. 17 Film cooling effectiveness on leading edge under rotating conditions, from Ahn *et al.* (2006)

in film cooling effectiveness due to the average effect of the unsteady wake (Fig.13).

3.3. Leading Edge

Gao and Han (2009) reported shower-head film cooling effectiveness measurements (using the PSP method) for a stationary model blade in a low speed wind-tunnel. Leading edges with up to seven rows (Fig.14) of radial and compound angled shaped and cylindrical holes were studied using the PSP method. Blowing ratios studied range from 0.5 to 2.0 with DR = 1.0. A mainstream turbulence intensity of 7% was maintained.

Results (Fig.14) showed that radial angles performed better than compound angles; shaped holes performed better than cylindrical holes for the range studied. The benefits of using a seven hole layout (over a three hole layout) are also evident - even when the same amount of coolant is used.

3.4. Blade Tip

Ahn *et al.* (2005) reported film cooling effectiveness values (using the PSP method) on a high pressure turbine blade tip tested in a blow-down facility. The holes in consideration were radial (i.e., normal to the tip leakage flow). The effect of using a squealer on film cooling effectiveness was also tested. Increasing the blowing ratio resulted in better coolant coverage on the tip (i.e. higher effectiveness).

Mhetras *et al.* (2008a) used a model rotor blade (on a three

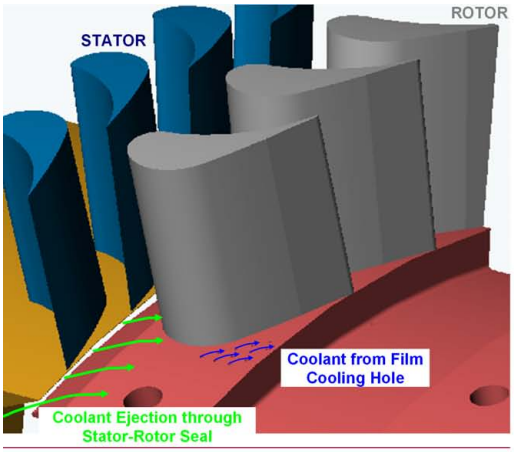

(a) Rotor-Stator Configuration with inclined slot

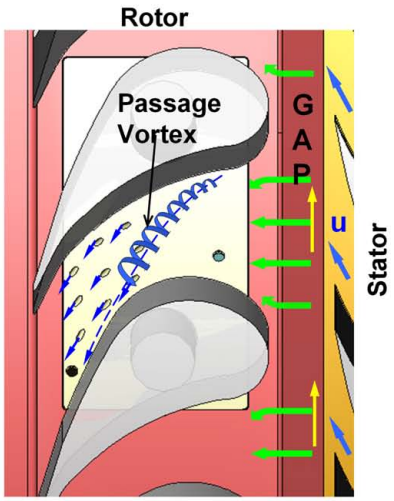

(b) Schematic of expected fluid mechanics in end-wall film cooling

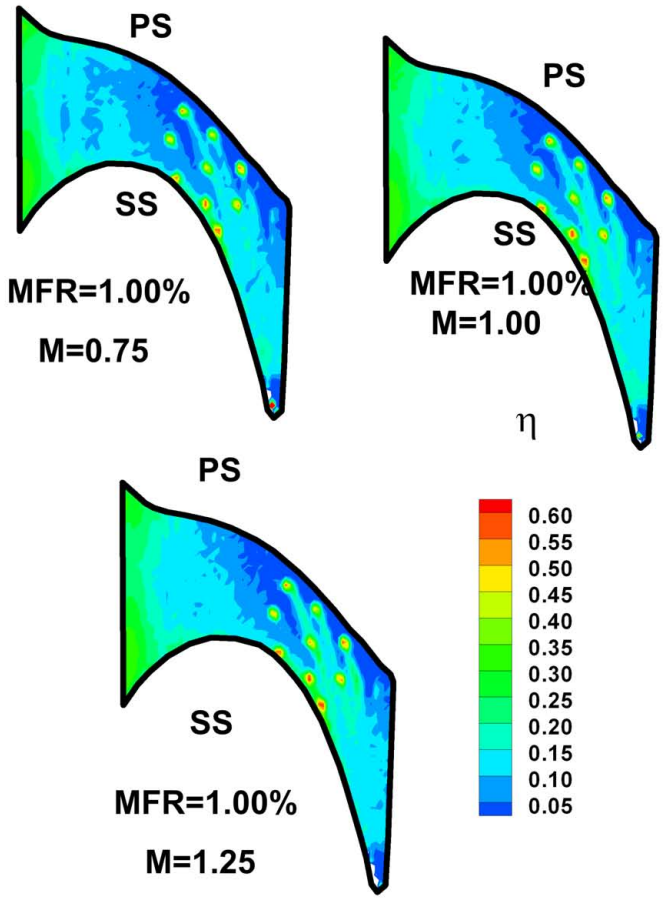

(c) Measured film cooling effectiveness values on end-wall under rotation

Fig. 18 Film cooling effectiveness on rotor end-wall under rotating conditions, from Suryanarayanan *et al.* (2007)

times scaled GE-E^3 2D blade profile) with a cut-back squealer tip to allow the film coolant accumulated on the tip to discharge, in the process cooling the trailing edge region of the tip. Inclined cylindrical holes (45^o) were used on the tip; radial and compound angled shaped holes were used on the near-tip region of the pressure side, as shown in Fig. 15. These tests (using the PSP method) were run in a four passage blow-down cascade, with an inlet Mach number of 0.23 and an exit Mach number of 0.67. The density ratio tested was 1.0 and the blowing ratios tested ranged from 0.5 to 2.0.

Results (Fig.15) show that for the tip film cooling holes, the effectiveness increases with blowing ratio. The cutback allows the coolant to flow over the trailing edge region, resulting in higher effectiveness. A blowing ratio of 1.0 seems optimal on for the holes on the near-tip region of pressure side, indicating that lift-off occurs at higher blowing ratios.

Gao *et al.* (2009b) studied the effect of the angle of attack on film cooling effectiveness (by the PSP technique) concluding that the results were fairly insensitive to the angle of attack.

3.5. Endwall

In a low-speed wind tunnel, Wright *et al.* (2007) compared the film cooling effectiveness downstream of rotor-stator slots with different seal geometries by the PSP technique. Using coolant (at 0.5% to 2% of mainstream passage mass flow rate) with DR = 1.0, it was concluded that using typical advanced rotor-stator seals *reduces* film cooling effectiveness compared with conventional inclined slots. Wright *et al.* (2008) used discrete film cooling holes in addition to the inclined slots to improve film coverage. Wright *et al.* (2009) tested the effect of upstream wakes generated by wake rods and delta wings to simulate the effect of upstream stator wakes and end-wall vortices, with the conclusion that the delta wings produce a larger negative effect on film cooling.

Gao *et al.* (2009a) ran tests on a turbine blade end-wall film-cooling under moderate Mach number conditions (Ma$_{in}$=0.27 and Ma$_{ex}$=0.44. Combined purge and discrete hole film cooling with DR = 1.0 was studied by the PSP technique. Tests were run using cylindrical holes as well as shaped holes. Results show that shaped holes offer significantly better coverage than cylindrical holes. The effect of hub secondary flows (horseshoe vortices etc.) on film cooling is evident from the film cooling effectiveness con-

tours. (Fig.16).

3.6. Effect of Rotation

Film cooling effectiveness under rotating conditions has been measured using a three stage multipurpose research turbine at the Turbomachinery Performance and Flow Research Laboratory at Texas A&M University, detailed in Schobeiri *et al.* (2000).

Leading Edge. Ahn *et al.* (2006) reported film cooling effectiveness on the leading edge of a rotating blade at the design condition of 2500rpm and two off design conditions of 2400rpm and 3000rpm. A boroscope was inserted between the trailing edge of the stationary stator vane and the rotating rotor vane. A laser routed through the boroscope (Fig.17) was used to excite the PSP, and a CCD camera (also routed through the boroscope) was used to capture the emitted long wavelength light. A DR of 1.0 (Nitrogen) was tested, with blowing ratios ranging from 0.5 to 2.0.

Ahn *et al.* (2006) used two rows of shower-head holes, one on the suction side and the other on the pressure side. Results (Fig.17) showed that the film cooling effectiveness was sensitive to the location of the stagnation line. When running at design condition (2550rpm), the stagnation line was such that coolant would be uniformly dispersed onto the suction and pressure sides. At the positive off-design condition (2400rpm), coolant from both the rows of cooling holes flows on to the suction side - and for the negative off-design condition (3000rpm), coolant was found to flow onto the pressure side, due to the shift in stagnation location due to variation in angle of attack. Similar results were reported for a blade with three rows of leading edge holes by Ahn *et al.* (2007).

Hub End-wall. The effect of rotation on the film cooling effectivness on the end-wall has been studied by Suryanarayanan *et al.* (2009), due to coolant discharged rotor-stator purge slot. Suryanarayanan *et al.* (2007) studied the combined film cooling effectiveness due to the purge slot and discrete holes under rotating conditions. Their test is discussed below:

The slot was inclined at 25^o to the mainstream, with a coolant to mainstream mass flow flow ratio of 1%. Discrete cylindrical hole film cooling is used to provide additional coverage in the passage. Tests were performed at three speeds: 2400rpm, 2550rpm and 3000rpm. Results (Fig.18) indicated that a blowing ratio of around 1.0 was optimal. Film cooling coverage was also found to be optimal at the design condition of 2550 rpm. Off design conditions seemed to result in a lowering of film cooling coverage. Also evident are the effects of the passage vortex, as can be seen by the angle of the film coolant traces.

4. CONCLUDING REMARKS

The pressure sensitive paint mass transfer analogy is a powerful method of acquiring film cooling effectiveness data in very complicated geometries. Data acquired is of very high quality and does not suffer from the dispersion due to thermal conduction in regions of high thermal gradients (such as those near holes).

Film cooling involves the measurement two parameters - film cooling effectiveness (η) and heat transfer coefficients (h). An attractive area for future research is to develop non-contact methods to measure heat transfer coefficients without suffering conduction effects - possibly using a heat/mass transfer or heat/momentum transfer analogy. A vast reliable database of results detailing heat transfer coefficients in different configurations, akin to the film cooling effectiveness database presented here will prove to be of immense value to the engine designer.

Investigations in the future could focus on the effect of velocity, temperature and turbulence profiles exiting the combustion chamber on film cooling of surface and end-walls of the first high pressure vane.

The effect of rotation and unsteady velocity and temperature profiles and stator wakes on rotor blade film cooling effectiveness and heat transfer coefficients is a relatively unexplored subject. Effects of thermal barrier coating spallation, film cooling hole blockage and surface roughness on the blade surface, end-walls and tip also merit investigation.

Gas turbine vane and blade designs are beginning to incorporate contoured end-walls to reduce aerodynamic losses associated with secondary vortices. The effect of contoured end-walls on film cooling can also be explored.

NOMENCLATURE

$A(T)$	Stern-Volmer Coefficient
$B(T)$	Stern-Volmer Coefficient
C	Mass Fraction
D	Mass Diffusion Coefficient (m^2/s)
DR	Coolant to Mainstream Density Ratio
G	Mass Flux ($kg/m^2 - s$)
Le	Lewis Number, α/D
M	Coolant to Mainstream Mass Flux Ratio
Ma	Mach Number
P	Total Pressure (Pa)
P_{O_2}	Partial Pressure of component (here, oxygen) (Pa)
T	Temperature (K)
W	Molecular Weight ($kg/k - mol$)
x	x co-ordinate (m)
$X_{O_2,fg}$	Mole fraction
y	y co-ordinate (m)
Greek Symbols	
α	Thermal diffusivity (m^2/s)
δ_f	Thickness of film (m)
η	Film cooling effectiveness
ϵ	Turbulent Diffusivity
ρ	Density (kg/m^3)
Subscripts	
∞	Pertaining to mainstream (outside film)
air	Pertaining to air
aw	Adiabatic Wall
C	Coolant inside hole
f	Pertaining to film
fg	Pertaining to foreign gas
M	Pertaining to mass transfer
mix	Mixture of air and foreign gas inside film
O_2	Pertaining to Oxygen
R	Reference
T	Turbulent or Thermal, depending on context
w	Wall
x	Pertaining to x co-ordinate direction
y	Pertaining to y co-ordinate direction

REFERENCES

Abhari, R., and Epstein, A., 1994, "An experimental study of film cooling in a rotating transonic turbine," *Journal of turbomachinery*, **116**, 63, DOI: 10.1115/1.2928279.

Ahn, J., Mhetras, S., and Han, J.C., 2005, "Film-Cooling Effectiveness on a Gas Turbine Blade Tip Using Pressure-Sensitive Paint," *Journal of Heat Transfer*, **127**, 521–530, DOI: 10.1115/1.1909208.

Ahn, J., Schobeiri, M., Han, J.C., and Moon, H., 2006, "Film cooling effectiveness on the leading edge region of a rotating turbine blade with two rows of film cooling holes using pressure sensitive paint," *Journal of Heat Transfer*, **128**, 879–888.

Ahn, J., Schobeiri, M., Han, J.C., and Moon, H., 2007, "Film cooling effectiveness on the leading edge region of a rotating blade using pressure sensitive paint," *International Journal of Heat and Mass Transfer*, **50**, 15–25, DOI: 10.1016/j.ijheatmasstransfer.2006.06.028.

Barigozzi, G., Franchini, G., and Perdichizzi, A., 2007, "End-Wall Film Cooling Through Fan-Shaped Holes With Different Area Ratios," *Journal of Turbomachinery*, **129**, 212, DOI: 10.1115/1.2464140.

Bindon, J.P., 1989, "The Measurement and Formation of Tip Clearance Loss," *Journal of Turbomachinery*, **111**(3), 257–263, DOI: 10.1115/1.3262264.

Bogard, D., and Thole, K., 2006, "Gas turbine film cooling," *Journal of Propulsion and Power*, **22**(2), 249–270, DOI: 10.2514/1.18034.

Bons, J., MacArthur, C., and Rivir, R., 1996, "The effect of high free-stream turbulence on film cooling effectiveness," *Journal of Turbomachinery*, **118**, 814, DOI: 10.1115/1.2840939.

Bunker, R., 2002, "Film Cooling Effectiveness Due to Discrete Holes Within a transverse Surface Slot," *ASME Paper GT-2002-30178*.

Bunker, R., 2005, "A review of shaped hole turbine film-cooling technology," *Journal of Heat Transfer*, **127**, 441, DOI: 10.1115/1.1860562.

Burd, S., CJ, S., and TJ, S., 2000, "Effect of slot bleed injection over a contoured end wall on nozzle guide vane cooling performance: Part II - Thermal measurements," *American Society of Mechanical Engineers Turbo Expo, 2000-GT-200*.

Cakan, M., and Taslim, M., 2007, "Experimental and Numerical Study of Mass/Heat Transfer on an Airfoil Trailing-Edge Slots and Lands," *Journal of Turbomachinery*, **129**, 281, DOI: 10.1115/1.2436898.

Charbonnier, D., Ott, P., Jonsson, M., Cottier, F., and Kobbe, T., 2009, "Experimental and numerical study of the thermal performance of a film cooled turbine platform," *Proceedings of Turbo Expo 2009 Paper: GT2009-60306*, Orlando, FL, United states.

Chen, P., Hung, M., and Ding, P., 2001, "Film cooling performance on curved walls with compound angle hole configuration," *Annals of the New York Academy of Sciences*, **934**, 353–360.

Chen, S.P., Li, P.W., Chyu, M.K., Cunha, F.J., and Abdel-Messeh, W., 2006, "Heat transfer in an airfoil trailing edge configuration with shaped pedestals mounted internal cooling channel and pressure side cutback," vol. 3 PART A, 819 – 828, Barcelona, Spain.

Choi, J., Mhetras, S., Han, J.C., Lau, S.C., and Rudolph, R., 2008, "Film Cooling and Heat Transfer on Two Cutback Trailing Edge Models With Internal Perforated Blockages," *Journal of Heat Transfer*, **130**(1), 012201 (pages 13), DOI: 10.1115/1.2780174.

Christophel, J.R., Thole, K.A., and Cunha, F.J., 2005, "Cooling the Tip of a Turbine Blade Using Pressure Side Holes—Part I: Adiabatic Effectiveness Measurements," *Journal of Turbomachinery*, **127**(2), 270–277, DOI: 10.1115/1.1812320.

Colban, W., Thole, K.A., and Haendler, M., 2008, "A Comparison of Cylindrical and Fan-Shaped Film-Cooling Holes on a Vane Endwall at Low and High Freestream Turbulence Levels," *Journal of Turbomachinery*, **130**(3), 031007 (pages 9), DOI: 10.1115/1.2720493.

Cunha, F., Dahmer, M., and Chyu, M., 2006, "Analysis of Airfoil Trailing Edge Heat Transfer and Its Significance in Thermal-Mechanical Design and Durability," *Journal of Turbomachinery*, **128**, 738, DOI: 10.1115/1.2220047.

Dhungel, A., Lu, Y., Phillips, W., Ekkad, S.V., and Heidmann, J., 2007, "Film cooling from a row of holes supplemented with anti vortex holes," *American Society of Mechanical Engineers Turbo Expo, Montreal , Canada, GT2007-27419*.

Dittmar, J., Schulz, A., and Wittig, S., 2002, "Assessment of various film cooling configurations using shaped and compound angle holes based on large scale experiments," *American Society of Mechanical Engineers Turbo Expo, GT2002-30176*.

Dring, R., Blair, M., and Joslyn, H., 1980, "An experimental investigation of film cooling on a turbine rotor blade," *Transactions of the ASME Journal of Engineering for Power*, **102**(1), 81 – 7.

Du, H., Ekkad, S., and Han, J.C., 1997, "Effect of unsteady wake with trailing edge coolant ejection on detailed heat transfer coefficient distributions for a gas turbine blade," *Journal of Heat Transfer*, **119**, 242, DOI: 10.1115/1.2824216.

Ekkad, S., Han, J.C., and Du, H., 1998, "Detailed film cooling measurements on a cylindrical leading edge model: effect of free-stream turbulence and coolant density," *Journal of turbomachinery*, **120**, 799, DOI: 10.1115/1.2841792.

Ekkad, S., Zapata, D., and Han, J.C., 1997, "Film Effectiveness Over a Flat Surface With Air and CO2 Injection Through Compound Angle Holes Using a Transient Liquid Crystal Image Method," *Journal of Turbomachinery*, **119**, 587.

Ethridge, M.I., Cutbirth, J.M., and Bogard, D.G., 2001, "Scaling of Performance for Varying Density Ratio Coolants on an Airfoil With Strong Curvature and Pressure Gradient Effects," *Journal of Turbomachinery*, **123**(2), 231–237, DOI: 10.1115/1.1343457.

Falcoz, C., Weigand, B., and Ott, P., 2006, "A comparative study on showerhead cooling performance," *International Journal of Heat and Mass Transfer*, **49**(7-8), 1274–1286.

Friedrichs, S., Hodson, H.P., and Dawes, W.N., 1996, "Heat Transfer Committee Best Paper of 1995 Award: Distribution of Film-Cooling Effectiveness on a Turbine Endwall Measured Using the Ammonia and Diazo Technique," *Journal of Turbomachinery*, **118**(4), 613–621, DOI: 10.1115/1.2840916.

Funazaki, K., Yokota, M., and Yamawaki, S., 1997, "Effect of periodic wake passing on film effectiveness of discrete cooling holes around the leading edge of a blunt body," *Journal of Turbomachinery*, **119**(2), 292–301, DOI: 10.1115/1.2841112.

Gao, Z., Narzary, D., and Han, J.C., 2009a, "Turbine Blade Platform Film Cooling With Typical Stator-Rotor Purge Flow and Discrete-Hole Film Cooling," *Journal of Turbomachinery*, **131**, 041004, DOI: 10.1115/1.3068327.

Gao, Z., Narzary, D., Mhetras, S., and Han, J.C., 2009b, "Effect of Inlet Flow Angle on Gas Turbine Blade Tip Film Cooling," *Journal of Turbomachinery*, **131**, 031005, DOI: 10.1115/1.2987235.

Gao, Z., Narzary, D., and Han, J.C., 2008, "Film cooling on a gas turbine blade pressure side or suction side with axial shaped holes," *International Journal of Heat and Mass Transfer*, **51**(9-10), 2139–2152, DOI: 10.1016/j.ijheatmasstransfer.2007.11.010.

Gao, Z., Narzary, D., and Han, J.C., 2009c, "Film-Cooling on a Gas Turbine Blade Pressure Side or Suction Side With Compound Angle Shaped Holes," *Journal of Turbomachinery*, **131**, 011019, DOI: 10.1115/1.2813012.

Gao, Z., and Han, J.C., 2009, "Influence of Film-Hole Shape and Angle on Showerhead Film Cooling Using PSP Technique," *Journal of Heat Transfer*, **131**(6), 061701 (pages 11), DOI: 10.1115/1.3082413.

Garg, V., 2000, "Heat transfer on a film-cooled rotating blade," *International Journal of Heat and Fluid Flow*, **21**(2), 134–145, DOI: 10.1016/S0142-727X(99)00072-7.

Goldstein, R.J., Eckert, E.R.G., and Burggraf, F., 1974, "Effects of hole geometry and density on three-dimensional film cooling," *International Journal of Heat and Mass Transfer*, **17**(5), 595 – 607, DOI: 10.1016/0017-9310(74)90007-6.

Goldstein, R.J., and Jin, P., 2001, "Film Cooling Downstream of a Row of Discrete Holes With Compound Angle," *Journal of Turbomachinery*, **123**(2), 222–230, DOI: 10.1115/1.1344905.

Goldstein, R.J., and Spores, R.A., 1988, "Turbulent Transport on the Endwall in the Region Between Adjacent Turbine Blades," *Journal of Heat Transfer*, **110**(4a), 862–869, DOI: 10.1115/1.3250586.

Goldstein, R., 1971, "Film cooling," *Advances in Heat Transfer*, **7**, 321–379.

Gritsch, M., Schulz, A., and Wittig, S., 1998, "Adiabatic wall effectiveness measurements of film-cooling holes with expanded exits," *Journal of Turbomachinery*, **120**, 549.

Han, J.C., Dutta, S., and Ekkad, S., 2000, *Gas turbine heat transfer and cooling technology*, Taylor and Francis, New York, NY 10001.

Han, J.C., and Ekkad, S., 2001, "Recent development in turbine blade film cooling," *International Journal of Rotating Machinery*, **7**(1), 21–40, DOI: 10.1155/S1023621X01000033.

Harasgama, S.P., and Burton, C.D., 1992, "Film Cooling Research on the Endwall of a Turbine Nozzle Guide Vane in a Short Duration Annular Cascade: Part 1—Experimental Technique and Results," *Journal of Turbomachinery*, **114**(4), 734–740, DOI: 10.1115/1.2928026.

Heidmann, J., Lucci, B., and Reshotko, E., 2001, "An experimental study of the effect of wake passing on turbine blade film cooling," *Journal of Turbomachinery*, **123**, 214.

Ito, S., Goldstein, R.J., and Eckert, E.R.G., 1978, "Film Cooling of a Gas Turbine Blade," *ASME Journal of Engineering for Power*, **100**, 476–481.

Jabbari, M.Y., Marston, K.C., Eckert, E.R.G., and Goldstein, R.J., 1996, "Film Cooling of the Gas Turbine Endwall by Discrete-Hole Injection," *Journal of Turbomachinery*, **118**(2), 278–284, DOI: 10.1115/1.2836637.

Jones, T., 1999, "Theory for the use of foreign gas in simulating film cooling," *International Journal of Heat and Fluid Flow*, **20**(3), 349–354.

Kays, W., Crawford, M., and Weigand, B., 2005, *Convective Heat and Mass Transfer*, McGraw-Hill.

Kim, Y.W., Downs, J.P., Soechting, F.O., Abdel-Messeh, W., Steuber, G.D., and Tanrikut, S., 1995, "Darryl E. Metzger Memorial Session Paper: A Summary of the Cooled Turbine Blade Tip Heat Transfer and Film Effectiveness Investigations Performed by Dr. D. E. Metzger," *Journal of Turbomachinery*, **117**(1), 1–11, DOI: 10.1115/1.2835638.

Kusterer, K., Bohn, D., Sugimoto, T., and Tanaka, R., 2007, "Double-Jet Ejection of Cooling Air for Improved Film Cooling," *Journal of Turbomachinery*, **129**(4), 809–815, DOI: 10.1115/1.2720508.

Kwak, J.S., and Han, J.C., 2003a, "Heat Transfer Coefficients and Film-Cooling Effectiveness on a Gas Turbine Blade Tip," *Journal of Heat Transfer*, **125**(3), 494–502, DOI: 10.1115/1.1565096.

Kwak, J., and Han, J.C., 2003b, "Heat transfer coefficients and film cooling effectiveness on the squealer tip of a gas turbine blade," *Journal of Turbomachinery*, **125**, 648.

Langston, L., 1980, "Crossflows in a turbine cascade passage," *ASME Journal of Engineering For Power*, **102**, 866–874, DOI: 10.1115/1.3230352.

Ligrani, P.M., Wigle, J.M., Ciriello, S., and Jackson, S.M., 1994a, "Film-Cooling From Holes With Compound Angle Orientations: Part 1—Results Downstream of Two Staggered Rows of Holes With 3d Spanwise Spacing," *Journal of Heat Transfer*, **116**(2), 341–352, DOI: 10.1115/1.2911406.

Global Digital Central
ISSN: 2151-8629

Ligrani, P., Wigle, J., and Jackson, S., 1994b, "Film-cooling from holes with compound angle orientations. Part 2: Results downstream of a single row of holes with 6d spanwise spacing," *ASME Transactions Journal of Heat Transfer*, **116**, 353–362, DOI: 10.1115/1.2911407.

Liu, T., Guille, M., and Sullivan, J., 2001, "Accuracy of pressure-sensitive paint," *AIAA journal*, **39**(1), 103–112, DOI: 10.2514/2.1276.

Luckey, D., Winstanley, D., Hanus, G., and L'Ecuyer, M., 1977, "Stagnation region gas film cooling for turbine blade leading-edge applications," *AIAA Journal of Aircraft*, **14**, 494–501, DOI: 10.2514/3.58806.

Martini, P., and Schulz, A., 2004, "Experimental and numerical investigation of trailing edge film cooling by circular coolant wall jets ejected from a slot with internal rib arrays," *Journal of Turbomachinery*, **126**, 229, DOI: 10.1115/1.1645531.

Martini, P., Schulz, A., and Bauer, H., 2006, "Film cooling effectiveness and heat transfer on the trailing edge cutback of gas turbine airfoils with various internal cooling designs," *Journal of Turbomachinery*, **128**, 196, DOI: 10.1115/1.2103094.

Mayle, R., 1991, "The role of laminar-turbulent transition in gas turbine engines," *Journal of Turbomachinery*, **113**, 509–537, DOI: 10.1115/1.2929110.

Mehendale, A., and Han, J.C., 1992, "Influence of high mainstream turbulence on leading edge film cooling heat transfer," *Journal of turbomachinery*, **114**, 707, DOI: 10.1115/1.2928023.

Mehendale, A., Han, J.C., Ou, S., and Lee, C., 1994, "Unsteady wake over a linear turbine blade cascade with air and CO2 film injection: Part IIŮeffect on film effectiveness and heat transfer distributions," *Journal of Turbomachinery*, **116**, 730, DOI: 10.1115/1.2929466.

Mhetras, S., Narzary, D., Gao, Z., and Han, J.C., 2008a, "Effect of a Cutback Squealer and Cavity Depth on Film-Cooling Effectiveness on a Gas Turbine Blade Tip," *Journal of Turbomachinery*, **130**, 021002, DOI: 10.1115/1.2776949.

Mhetras, S., and Han, J.C., 2006, "Effect of superposition on spanwise film-cooling effectiveness distribution on a gas turbine blade," *Proc. ASME IMECE, Heat Transfer Division, (Publication) HTD, Paper No: IMECE2006-15084*, Chicago, IL, United states.

Mhetras, S., Han, J.C., and Rudolph, R., 2007, "Effect of flow parameter variations on full coverage film-cooling effectiveness distribution on a gas turbine blade with compound shaped holes," *Proceedings of the ASME Turbo Expo 2007, Paper GT2007-27071*, Montreal, Canada.

Mhetras, S., Han, J.C., and Rudolph, R., 2008b, "Film-cooling effectiveness from shaped fulm cooling holes for a gas turbine blade," *Proceedings of the ASME Turbo Expo 2008, Paper GT2008-50916*, Berlin, Germany.

Mick, W., and Mayle, R., 1988, "Stagnation film cooling and heat transfer, including its effect within the hole pattern," *Journal of Turbomachinery*, **110**, 66, DOI: 10.1115/1.3262169.

Moffat, R., 1987, "Turbine blade cooling," *Heat transfer and fluid flow in rotating machinery; Proc. First International Symposium on Transport Phenomena, Honolulu, HI, Apr. 28-May 3*, 3–26.

Narzary, D.P., Liu, K.C., Rallabandi, A.P., and Han, J.C., 2010, "Influence of Coolant Density on Turbine Blade Film-Cooling Using Pressure Sensitive Paint Technique," *Proceedings of the ASME Turbo Expo, Paper GT2010-22781*, Glasgow, Scotland.

Narzary, D.P., Liu, K.C., and Han, J.C., 2009, "Influence of coolant density on turbine blade platform film-cooling," *American Society of Mechanical Engineers Turbo Expo, GT2009-59342*.

Narzary, D., Gao, Z., Mhetras, S., and Han, J.C., 2007, "Effect of unsteady wake on film-cooling effectiveness distribution on a gas turbine blade with compound shaped holes," *Proceedings of the ASME Turbo Expo 2007, Paper GT2007-27070*, Montreal, Canada.

Nicoll, W., and Whitelaw, J., 1967, "The effectiveness of the uniform density, two- dimensional wall jet(Two-dimensional wall jet effectiveness measurements and calculation procedures for injection conditions)," *International Journal of Heat and Mass Transfer*, **10**, 623–639, DOI: 10.1016/0017-9310(67)90109-3.

Oke, R., Simon, T., Shih, T., Zhu, B., Lin, Y., and Chyu, M., 2002, "Film cooling experiments with flow introduced upstream of a first stage nozzle guide vane through slots of various geometries," *American Society of Mechanical Engineers Turbo Expo, GT2002-30169*.

Pedersen, D., Eckert, E., and Goldstein, R., 1977, "Film cooling with large density diffferences between the mainstream and the secondary fluid measured by the heat-mass transfer analogy," *ASME Transactions Journal of Heat Transfer*, **99**, 620–627.

Rallabandi, A.P., Grizzle, J., and Han, J.C., 2008, "Effect of upstream step on flat plate film cooling effectiveness using PSP," *2008 Proceedings of the ASME Summer Heat Transfer Conference, HT08-56194*, vol. 2, 599 – 609, Jacksonville, FL, United states.

Rallabandi, A.P., Li, S.J., and Han, J.C., 2010, "Unsteady wake and coolant density effects on turbine blade film cooling using PSP technique," *ASME IHTC 14, Washington DC, USA, IHTC14-22911*, Washington, DC, United states.

Reiss, H., and Bölcs, A., 2000, "Experimental study of showerhead cooling on a cylinder comparing several configurations using cylindrical and shaped holes," *Journal of Turbomachinery*, **122**, 161, DOI: 10.1115/1.555420.

Rigby, M., Johnson, A., and Oldfield, M., 1990, "Gas turbine rotor blade film cooling with and without simulated NGV shock waves and wakes," GT78 8p, Brussels, Belg.

Schmidt, D., Sen, B., and Bogard, D., 1996, "Film cooling with compound angle holes: adiabatic effectiveness," *Journal of Turbomachinery*, **118**, 807, DOI: 10.1115/1.2840938.

Schobeiri, M., Gilarranz, J., and Johansen, E., 2000, "Aerodynamic and Performance Studies of a Three Stage High Pressure Research Turbine with 3-D-Blades, Design Points and Off-Design Experimental Investigations," *Proceedings of ASME Turbo-Expo, Paper: 2000-GT-484*.

Schwarz, S.G., Goldstein, R.J., and Eckert, E.R.G., 1991, "The Influence of Curvature on Film Cooling Performance," *Journal of Turbomachinery*, **113**(3), 472–478, DOI: 10.1115/1.2927898.

Sinha, A.K., Bogard, D., and Crawford, M., 1991, "Film-Cooling Effectiveness Downstream of a Single Row of Holes With Variable Density Ratio," *Journal of Turbomachinery*, **113**(3), 442–449, DOI: 10.1115/1.2927894.

Suryanarayanan, A., Mhetras, S.P., Schobeiri, M.T., and Han, J.C., 2009, "Film-Cooling Effectiveness on a Rotating Blade Platform," *Journal of Turbomachinery*, **131**(1), 011014 (pages 12), DOI: 10.1115/1.2752184.

Suryanarayanan, A., Ozturk, B., Schobeiri, M., and Han, J.C., 2007, "Film-cooling effectiveness on a rotating turbine platform using pressure sensitive paint technique," *Proceedings of the ASME Turbo Expo, Paper GT2007-27122*, Montreal, Que., Canada.

Takeishi, K., Aoki, S., Sato, T., and Tsukagoshi, K., 1992, "Film cooling on a gas turbine rotor blade," *Journal of turbomachinery*, **114**, 828, DOI: 10.1115/1.2928036.

Takeishi, K., Matsuura, M., Aoki, S., and Sato, T., 1990, "An Experimental Study of Heat Transfer and Film Cooling on Low Aspect Ratio Turbine Nozzles," *Journal of Turbomachinery*, **112**(3), 488–496, DOI: 10.1115/1.2927684.

Taslim, M., Spring, S., and Mehlman, B., 1992, "Experimental investigation of film cooling effectiveness for slots of various exit geometries," *Journal of Thermophysics and Heat Transfer*, **6**(2), 302–307, DOI: 10.2514/3.359.

Teng, S., Sohn, D., and Han, J.C., 2000, "Unsteady wake effect on film temperature and effectiveness distributions for a gas turbine blade," *Journal of Turbomachinery*, **122**, 340, DOI: 10.1115/1.555457.

Waye, S., and Bogard, D., 2007, "High-Resolution Film Cooling Effectiveness Measurements of Axial Holes Embedded in a Transverse Trench With Various Trench Configurations," *Journal of Turbomachinery*, **129**, 294, DOI: 10.1115/1.2464141.

Wright, L.M., Gao, Z., Varvel, T.A., and Han, J.C., 2005, "Assessment of steady state PSP, TSP, and IR measurement techniques for flat plate film cooling," *Proceedings of the ASME Summer Heat Transfer Conference, Paper: HT2005-72363*, San Francisco, CA, United states.

Wright, L., Blake, S., and Han, J.C., 2007, "Effectiveness Distributions on Turbine-Blade Cascade Platforms Through Simulated Stator-Rotor Seals," *Journal of thermophysics and heat transfer*, **21**(4), 754, DOI: 10.2514/1.30382.

Wright, L., Blake, S., Han, J.C., *et al.*, 2008, "Film Cooling Effectiveness Distributions on a Turbine Blade Cascade Platform With Stator-Rotor Purge and Discrete Film Hole Flows," *Journal of Turbomachinery*, **130**, 031015, DOI: 10.1115/1.2777186.

Wright, L., Blake, S., Rhee, D., Han, J.C., *et al.*, 2009, "Effect of Upstream Wake With Vortex on Turbine Blade Platform Film Cooling With Simulated Stator-Rotor Purge Flow," *Journal of Turbomachinery*, **131**, 021017, DOI: 10.1115/1.2952365.

Zhang, L., and Fox, M., 1999, "Flat Plate Film Cooling Measurements using PSP Gas Chromatograph Techniques," *Proc. Fifth ASME/JSME Joint Thermal Engineering Conference, San Diego, CA*, ASME/JSME.

Zhang, L., and Jaiswal, R., 2001, "Turbine nozzle endwall film cooling study using Pressure-Sensitive Paint," *Journal of Turbomachinery*, **123**, 730, DOI: 10.1115/1.1400113.